CHALMERS

Employing Realistic Propagation Maps for Resource Allocation Strategies in Cellular Networks

Master of Science Thesis

HAN ZHOU

Department of Signals and Systems
Division of Communication Systems
CHALMERS UNIVERSITY OF TECHNOLOGY
Göteborg, Sweden, 2011
Report No. EX021/2011

Employing Realistic Propagation Maps for Resource Allocation Strategies in Cellular Networks

Han Zhou

Supervisor: James Gross and Erik Agrell

Advisor: Nima Seifi and Farshad Naghibi

Department of Signals and Systems
Chalmers University of Technology
Gothenburg, Sweden

Mobile Network Performance Group
UMIC Research Centre
RWTH-Aachen University
Aachen, Germany
February,2011

Employing Realistic Propagation Maps for Resource Allocation Strategies in Cellular Networks

Han Zhou

Technical report No. EX021/2011
Department of Signals and Systems
Chalmers University of Technology
SE-412 96 Gothenburg
Sweden
Email: hanz@student.chalmers.se

Abstract

Within the last decade, Orthogonal Frequency Division Multiplexing(OFDM) has been considered as the most promising transmission and multiple-access scheme for the 4th generation of wireless networks including 3GPP LTE and WiMAX. OFDMA has the feature of flexibility in radio resource allocation as well as exploiting frequency and multi-user diversity. A key limitation of OFDM-based system is inter-cell interference, which exists if the same subcarriers are used by neighboring cells simultaneously, leading to degradation of network performance. Thus, various approaches such as power control, spatial techniques, interference cancellation techniques, new decoding algorithms and resource allocation have been introduced into multi-cell OFDMA networks leading to an active research area of inter-cell interference mitigation.

The objective of this thesis is to utilize the propagation maps for resource allocation in cellular networks and find an Adaptive Soft Frequency Reuse(ASFR) scheme for Inter-cell Interference(ICI) coordination which can improve the system performance. Propagation maps are a kind of pre-calculated data which provide information on average channel gains for different coordinates of a certain environment. Using these propagation maps and employing techniques such as Global Positioning System(GPS) to detect the position of a terminal in a network, signaling overhead and delays resulting from channel state feedbacks from terminals to base stations can be significantly reduced and it provides the system a possibility to be able to adapt to the change of traffic load.

In this thesis, a centralized multi-cell scheduling system is provided and the ICI coordination is modeled to maximize the worst user's performance based on the average channel gains. This model is found to be able to adapt to different distributions of the traffic load and improve overall system performance for the data stream traffic, such as Voice over Internet Protocol(VoIP).

Key Words — OFDMA, inter-cell interference coordination, propagation maps, adaptive soft frequency reuse.

Contents

List of Figures

List of Tables

Chapter 1

Introduction

The rapid growing of mobile data usage such as multimedia online gaming, mobile TV, web browsing and streaming contents leads to the demand of more advanced cellular system with higher spectral efficiency as well as lower latency. Although the peak data rate 1-10 Mb/s are advertised for the Third-Generation (3G) mobile network techniques such as EV-DO [3] and High Speed Packet Access (HSPA) [4], the general user experience is poor. All those drive a need for the 4th Generation (4G) networks to have a better network performance. Therefore, projects such as LTE [5] and Long Term Evolution Advanced (LTE-A) [6] are launched by the 3rd Generation Partnership Project (3GPP) in order to meet with the increasing wireless access requirements [7]. Similar to Worldwide Interoperability for Microwave Access (WiMAX), LTE and LTE-A are also based on Orthogonal Frequency Division Multiplexing (OFDM) technology [8], which is considered as a promising transmission and multiple-access scheme and brings considerable performance improvement.

Cellular networks are interference-limited due to the requirement of sharing the scarce spectrum for high-rate multimedia communication [9]. Interference is distinguished from noise in that the negative impact of general noise can be overcome by increasing the transmit power, whereas this simple approach degrades the performance of the neighboring devices by increasing the distortion of the received signals. In an OFDM-based system, since sub-carriers are orthogonal, interference mainly comes from neighboring cells that use the same sub-carriers simultaneously. Mobile users at cell edge usually suffer a lot from the Inter-cell Interference (ICI) compared with those at cell center. Therefore, it is important to mitigate the ICI from the overall system performance point of view.

One major alternative for ICI mitigation is ICI coordination [10], which aims at performing the down-link resource management in a coordinated way among cells. These coordinations can be either on the available time-frequency resources or on the transmit power applied on different radio resources. This kind of approach has potential possibilities for improvement in Signal to Interference and Noise Ratio (SINR), thus in throughput and coverage of the users at cell borders. There are three different major approaches for ICI coordination in OFDM based cellular system: Hard Frequency Reuse (HFR), Fractional Frequency Reuse (FFR) and Soft Frequency Reuse (SFR) (see Figure 1.1).

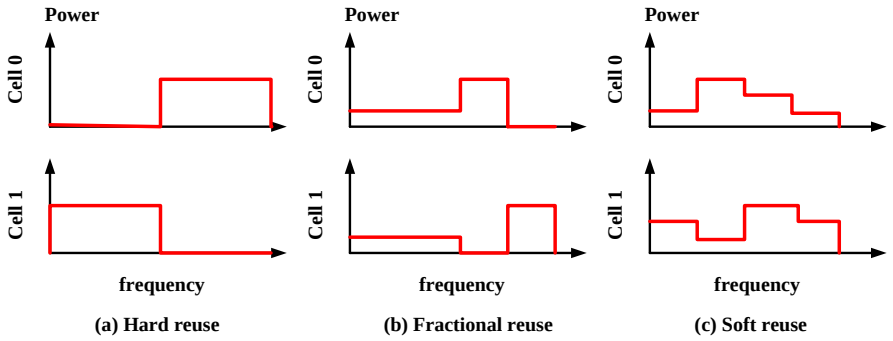

Figure 1.1: *ICI coordination schemes*

- HFR divides the system frequency bandwidth into several parts and allows neighboring cells using different bandwidths; it avoids the ICI by reduction of frequency reuse, which means less frequency diversity and spectral efficiency.

- FFR [11] splits the system frequency bandwidth into two parts: one part is for mobile users at cell borders and the other part is for those at cell center. A Mobile Station (MS) located at cell center which suffers less from ICI shares the frequency bandwidth with neighboring cells. MSs at cell borders use the other part of bandwidth which is not used by neighboring cells. In this way, FFR has the advantage of HFR to mitigate the negative impact of ICI on system performance, and meanwhile overcomes the HFR's disadvantage of low spectral efficiency (e.g. see [12] [13] [14] [15]). Mature technologies and good performance improvement in cell edge user throughput make FFR well-known and it is recommended for 4G Networks.

- SFR [16] [17] allows the overall frequency bandwidth is to be shared by all the cells in the networks to increase the spectral efficiency. In order to make ICI controllable, each sub-carrier is allocated with a different power setting.

In [16], SFR has been shown to have superior performance compared to HFR and FFR. However, most of the SFR schemes (such as [2], [18]) use static power allocation, which does not consider the changes of the traffic load. As the power allocation is highly dependent on the traffic load of the system and the distance between the receiver and signal source/interference source, a fixed power allocation can not be omnipotent for all the unpredictable conditions. Therefore, here comes the need for the dynamic SFR scheme.

In order to have a good dynamic SFR scheme, there are some challenges that researchers should confront, such as how to intelligently deal with different traffic loads and the distribution of the MSs. In addition, the power allocation is usually a non-linear optimization problem, which results in another challenge – the computational complexity to perform good power allocations. Hence, currently people are still looking for a good dynamic SFR scheme and SFR is one of the active ICI coordination research areas in the research community. The primary objective of this thesis is to investigate a good approach for practical dynamic SFR scheme assisted by the positioning technology and the pre-calculated propagation maps [1] (see Section 4.3.4) and evaluate how much improvement it can have since a positioning technology is employed for the ICI coordination to reduce the signaling overhead, the sensitivity to the inaccuracy of the positioning should also be investigated.

In this first chapter, a brief introduction to the subject of the thesis has been presented. The rest of the framework of this investigation is as following: in the second chapter, the basic theoretics that are used in this thesis are given. The third chapter is about the related work and the scope of the thesis. The fourth chapter is about the proposed scheme and system design. In the fifth chapter, the evaluation methodology is given which shows how the practical system is mapped to the simulations. The sixth chapter describes the evaluation scenarios and shows the simulation results. Finally, the thesis is ended with a summary.

[1] Propagation map: provides the average channel gain according to the position of a terminal.

Chapter 2

Theoretical Basics

2.1 Wireless channel characteristics

For all the reliable high-speed communications, the wireless radio channel is a severe challenge due to its attenuation of the transmitted signal. Generally, it is useful to model and distinguish the impacts of the channel in three ways – path loss, shadowing and fading [19]. Path loss is the effect of the dissipation of the power radiated by the transmitter as well as the effects of the propagation channel. Generally, it assumed to be a deterministic effect which is dependent on the distance between the transmitter and the receiver. Path loss is referred to as a large-scale propagation effect. Shadowing is another large-scale propagation effect due to the obstacles between the transmitter and receiver, which attenuate signal through absorption, reflection, scattering, and diffraction. Fading is referred to as small-scale propagation effect, which is due to the time delay and time-varying characteristics of a multipath channel; it has a stochastic nature as shadowing but it can lead to significant attenuation changes.

All these three impacts of the wireless channel result in the general attenuation of the radio channel. This overall attenuation is modeled in equation (2.1) [19]:

$$\alpha(t) = \alpha_{\mathrm{PL}}(t) \cdot \alpha_{\mathrm{SH}}(t) \cdot \alpha_{\mathrm{FA}}(t), \tag{2.1}$$

where $\alpha_{\mathrm{PL}}(t), \alpha_{\mathrm{SH}}(t)$ and $\alpha_{\mathrm{FA}}(t)$ are attenuations of path loss, shadowing and fading respectively.

Environment	Model Type	Antenna height(m)	γ range
Urban	LOS [1]	4	1.4
Urban	NLOS	4	2.8
Urban	LOS	12	2.5
Urban	NLOS	12	4.5
Suburban	LOS	12	2.5
Suburban	NLOS	5	3.4
Rural	LOS	55	3.3
Rural	NLOS	55	5.9

Table 2.1: *Parameters of the general path loss model from measurements in Finland for 5.3 GHz and a reference distance of 1 m, see [20]*

2.1.1 Path loss

The phenomenon of path loss is assumed to depend on the signal frequency and the distance between the transmitter and receiver. Usually, the path loss for propagating in free space over a distance d where no object obstructs the path between the transmitter and receiver can be calculated by Friis free space equation [21]:

$$\frac{P_{\mathrm{r}}}{P_{\mathrm{t}}} = (\frac{\lambda}{4\pi d})^2 \cdot G_{\mathrm{t}} \cdot G_{\mathrm{r}}, \tag{2.2}$$

in which P_{r} is received power, P_{t} is transmitted power, λ is the carrier's wavelength, G_{t} is the transmitter antenna gain, G_{r} is the receiver antenna gain, and d is the distance between the transmitter and receiver. However, generally, it is not the case that the signal propagates in the free space; there are reflections and scattering. For general analysis of various system designs, it is better to use simple path loss model that captures the essence to approximate the real case without using a complicated one. Therefore, the following simplified model is commonly used [22]:

$$L_{\mathrm{pathloss}}(\mathrm{dB}) = K(\mathrm{dB}) - 10 \cdot \gamma \cdot \log_{10}(\frac{d}{d_0}), \tag{2.3}$$

where K is a unit-less constant which depends on the antenna characteristics and

[1] LOS: line-of-sight, there are no obstructions between the transmitter and receiver and the signal propagates along a straight line.

the average channel attenuation, d_0 is a reference distance for the antenna far-field, and γ is the path loss exponent (see Table 2.1). The equation (2.3) is generally only valid with $d > d_0$. Sometimes, K is set to be the free space path loss at distance d_0:

$$K(\text{dB}) = -20\log_{10}(\frac{4\pi d_0}{\lambda}). \tag{2.4}$$

2.1.2 Shadowing

Shadowing is an abstraction that reflects the result of a sum of several propagation phenomena which occur when the signal propagates in an environment of blockage from objects in the signal path: reflections, diffraction, refraction, scattering and absorption. Since the location, size as well as the dielectric properties of the blocking objects determine the shadowing, it has a high correlation in space; the attenuation varies rather over longer time scales such as seconds if the transmitter or receiver are mobile. It is common to use statistical model to describe the variations. One of the common models is the log-normal distribution with the probability density function given as [22]:

$$p(\alpha_{\text{SH}}) = \frac{1}{\sigma_{\text{SH}}\sqrt{2\pi}} exp[-\frac{(\alpha_{\text{SH}} - \mu_{\text{SH}})^2}{2\sigma_{\text{SH}}^2}], \tag{2.5}$$

in which $\sigma_{\text{SH}}(\text{dB})$ is the standard deviation and $\mu_{\text{SH}}(\text{dB})$ is the mean of random variable – shadowing $\alpha_{\text{SH}}(\text{dB})$.

2.1.3 Fading

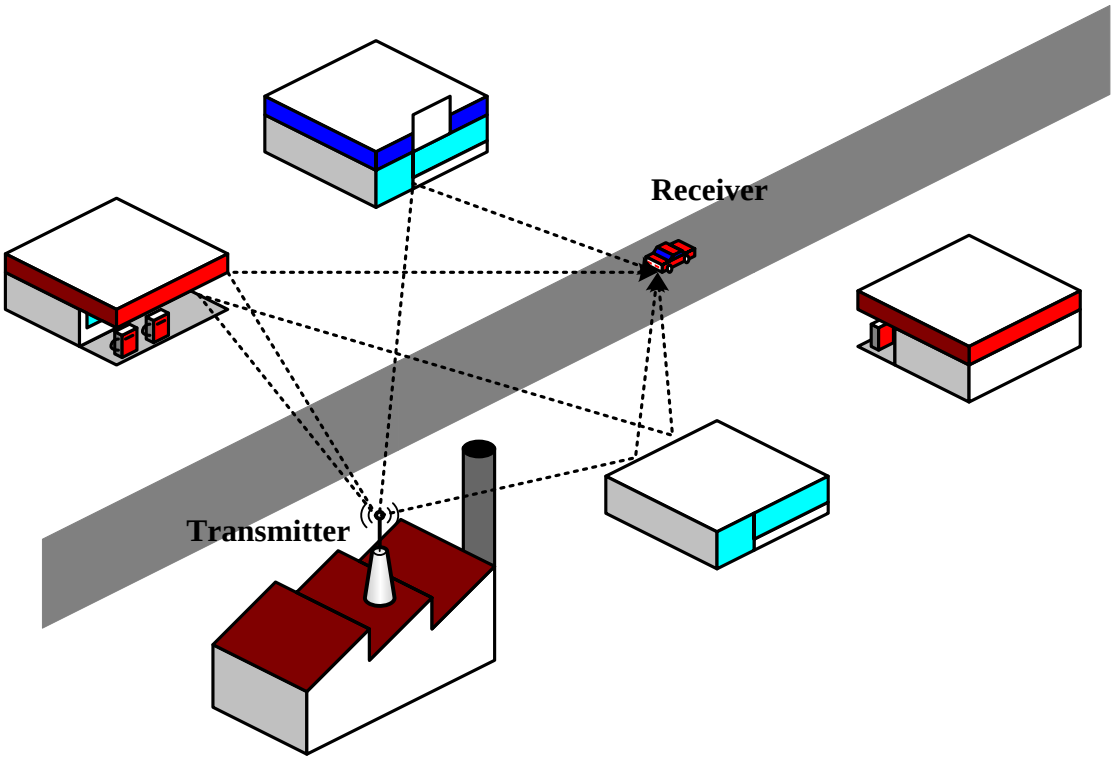

Figure 2.1: *Multipath propagation*

Figure 2.1 shows the basics of fading: signal arriving at the receiver has multiple copies due to the different paths. Before introducing the fading channel model, the symbols to be used later are denoted in Table 2.2. Typically each path i has a different path length $l_i(t)$ at time instant t leading to signal copies of different delays $\tau_i(t) = \frac{l_i(t)}{c}$, where c is the speed of light. Beside the multipath delay, since different copies pass through different obstacles (e.g. walls and windows made of different materials), each path i has a different absorption factor $a_i(t)$. In this way, the multipath environment introduces a constructive and destructive addition of multipath components. If the receiver is moving, since the propagation path changes, therefore, $a_i(t)$ and $\tau_i(t)$ change with experiencing different propagation environment. Most of the following is from [19] and [22].

Considering a bandpass signal with complex envelope $\overline{s}(t)$ at the carrier frequency f_c, the received signal $y(t)$ is given as following:

$$y(t) = Re(\sum_{\forall i} a_i(t) \cdot \overline{s}(t - \frac{l_i(t)}{c}) \cdot e^{2\pi j \cdot f_c \cdot (t - \frac{l_i(t)}{c})}) \tag{2.6}$$

Description	Symbols
Path no.	i
Instant time	t
Path i length	$l_i(t)$
Path i delay	$\tau_i(t)$
Absorption factor of path i	$a_i(t)$
Carrier frequency	f_c
Bandpass signal envelope at f_c	$\overline{s}(t)$
Received signal	$y(t)$
Phase shift at f_c	$\varphi_i(t)$
Doppler frequency	f_d
Doppler shift	ν_i
Signal arrival angle	θ_i
Channel impulse response	$c(\tau, t)$
Delay spread	$\Delta\tau$

Table 2.2: *Parameter Table for Fading Channel Model*

It is assumed that the received bandpass signal is given as:

$$y(t) = Re(\overline{y}(t) \cdot e^{2\pi j \cdot f_c t}). \tag{2.7}$$

Taking the mobility of the receiver into account and denoting the signal arrival angle by θ_i and the velocity by v_i, the received signal complex envelope $\overline{y}(t)$ is given as following:

$$\overline{y}(t) = \sum_{\forall i} a_i(t) \cdot e^{-j\varphi_i} \cdot e^{-2\pi j \cdot \cos(\theta_i) \cdot t \frac{v}{\lambda}} \cdot \overline{s}(t - \tau_i(t) + \frac{v_i \cdot \cos(\theta_i) \cdot t}{c}) \tag{2.8}$$

where $\lambda = \frac{c}{f_c}$ is the carrier wavelength, $\varphi_i(t) = 2\pi \cdot \frac{l_i(t)}{\lambda}$ is the phase shift of the carrier frequency. Then introduce the Doppler frequency $f_d = \frac{v}{\lambda}$ and Doppler shift $\nu_i = \cos(\theta_i) \cdot f_d$ and ignore $\frac{v_i \cdot \cos(\theta_i) \cdot t}{c}$, $\overline{y}(t)$ can be rewritten as:

$$\overline{y}(t) = \sum_{\forall i} a_i(t) \cdot e^{-j\varphi_i(t)} \cdot e^{2\pi j \cdot \nu_i \cdot t} \cdot \overline{s}(t - \tau_i(t)) \tag{2.9}$$

Therefore, the channel impulse response is derived as following:

$$c(\tau, t) = \sum_{\forall i} a_i(t) \cdot e^{-j\varphi_i(t)} \cdot e^{2\pi j \cdot \nu_i \cdot t} \cdot \delta(\tau - \tau_i(t)). \tag{2.10}$$

The Doppler spread phenomenon in frequency results in a time selective behavior of wireless channel. However, the delay spread[2] in time results in a frequency selective behavior. If coherent demodulation is assumed, processing time is the symbol length T_s, $n \cdot T_s$ represents the processing time span (as differential detection or an equalization process cause $n > 1$) and B is the bandwidth of the signal, then the fading channel can be characterized as Table 2.3 [19].

Criteria	**Fading Category**	**Description**
$B \cdot \Delta\tau \ll 1$	Flat fading	No significant pulse distortion
$B \cdot \Delta\tau \gg 1$	Frequency selective	Signal pulse distortion
$f_d \cdot n \cdot T_s \ll 1$	Slow fading	Time-invariant over a processing length
$f_d \cdot n \cdot T_s \gg 1$	Fast fading	Time-variant over a processing length

Table 2.3: *Characteristics of Fading Channel*

Generally, Rayleigh distribution with Clarke's spectrum is commonly used to describe the wireless fading channel. It is assumed that the complex channel gain has the variance δ_τ^2 and the magnitude of the complex gain has following Probability Density Function (PDF) [19]:

$$p(x) = \begin{cases} \frac{x}{\delta_\tau^2} \cdot exp(-\frac{x^2}{2\delta_\tau^2}), & x \geq 0; \\ 0, & x < 0. \end{cases} \tag{2.11}$$

Then the distribution of power z is χ^2 distribution with two degrees of freedom due to the two independent jointly Gaussian processes of the real and imaginary parts of the signal combining as following:

$$p(z) = \begin{cases} \frac{1}{2\delta_\tau^2} \cdot exp(-\frac{z}{2\delta_\tau^2}), & z \geq 0; \\ 0, & z < 0. \end{cases} \tag{2.12}$$

$C(\delta_\tau, f)$ which is the power spectrum of $c(\delta_\tau, t)$ is given:

$$C(\delta_\tau, f) = \frac{\delta_\tau^2}{\pi f_d \sqrt{1 - (\frac{\nu}{f_d})^2}}, |\nu| \leq f_d. \tag{2.13}$$

which is often referred as Jakes power spectrum [23], see figure 2.2.

[2]Delay spread: the difference between "earliest" and "latest" received signal copies.

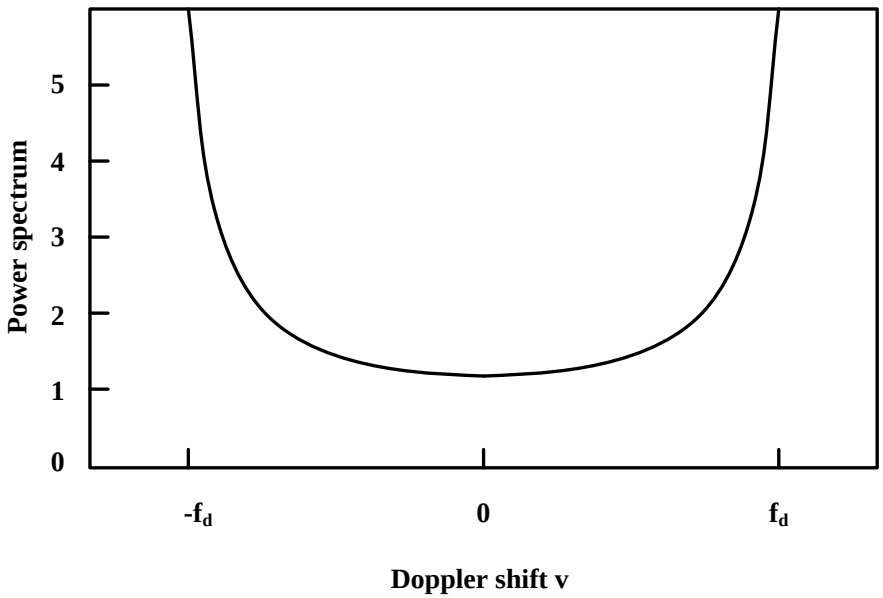

Figure 2.2: *Doppler power spectrum*

2.2 LTE network basics

3GPP LTE is the latest standard in the mobile network technology; it aims at increasing user throughputs, system capacity and reducing the latency, thus improving user experience with full mobility. In order to avoid going through every detail of LTE, here only those related with the thesis are summarized. Since one objective of 3GPP in developing the evolved packet system of LTE is to move towards a "packet only architecture" on the radio access network side as well as on the core network side, LTE is designed to be packet based and Internet Protocol (IP) is chosen to carry all the types of traffic [24].

2.2.1 Evolved packet system architecture

The architecture of evolved packet system (shown as Figure 2.3) consists of Evolved Packet Core (EPC) on the core network side and Evolved Universal Terrestrial Radio Access Network (E-UTRAN) on the Radio Access Network (RAN) side [25].

The E-UTRAN consists of only eNode (eNB)s, which are to support all the functions such as radio bearer control, mobility management, admission control and scheduling. Different eNBs are connected with each other via the X2 interface

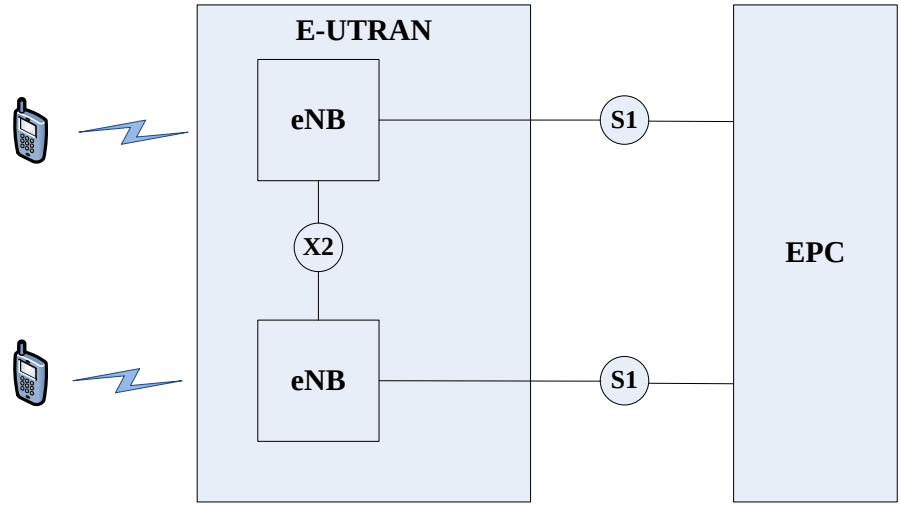

Figure 2.3: *Evolved packet system architecture*

which is a direct interface for handover and radio resource managements. These eNBs are also connected with EPC by S1 interface.

The EPC performs control plane functionality (mobility, user identities and security) and bearer-plane functionality (packets routing and forwarding, connectivity to external networks).

2.2.2 LTE radio interface architecture

Since the LTE protocol structure related to uplink is similar to the downlink, in this subsection, only a general overview of the LTE protocol architecture for the downlink is illustrated in Figure 2.4 [24].

Before transmission, the incoming IP packets should passed through multiple protocol entities:

- Packet Data Convergence Protocol (PDCP) performs IP header compression/decompression and it is also responsible for ciphering/deciphering the transmitted/received data.
- Radio Link Control (RLC) is responsible for segmentation/concatenation, retransmission handling, and in-sequence delivery to higher layers.

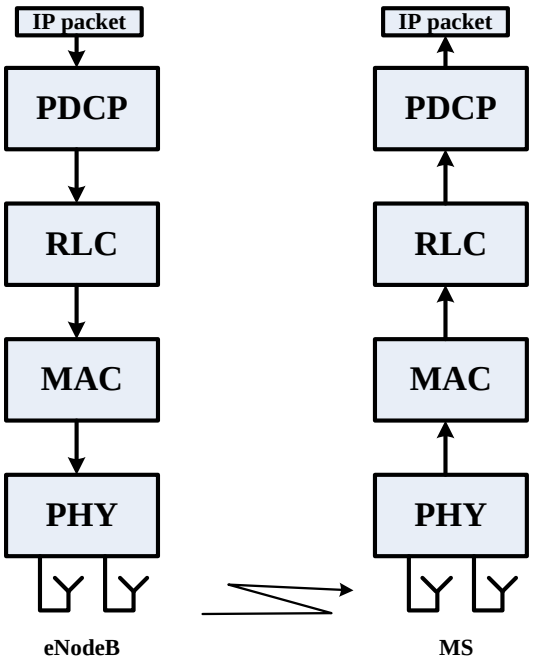

Figure 2.4: *LTE Protocol Structure (downlink)*

- Medium Access Control (MAC) is in charge of hybrid-ARQ retransmissions, uplink and downlink scheduling.
- Physical Layer (PHY) deals with coding/decoding, modulation/demodulation, multi-antenna mapping, and other physical layer functions.

2.2.3 LTE Frame & Duplex

Figure 2.5 shows the LTE frame structure for LTE transmission [26]: the LTE frame consists of 10 1ms-duration sub-frames and each sub-frame is divided into 2 0.5ms-duration slots. Moreover, every slot is composed of 6 or 7 OFDM symbols.[3] The spectral resources in LTE are allocated as a combination of both time and frequency units, denoted as Resource Block (RB). A RB consists of 12 adjacent sub-carriers with 7 OFDM symbols considering normal cyclic prefix [24].

LTE can operate in both Frequency Division Duplex (FDD) and Time Division Duplex (TDD) as shown in Figure 2.6. In FDD operation, uplink and downlink

[3]This is dependent on the cyclic prefix length; for normal cyclic prefix, each slot consists of 7 OFDM symbols, and for extended cyclic prefix, it is of 6 OFDM symbols.

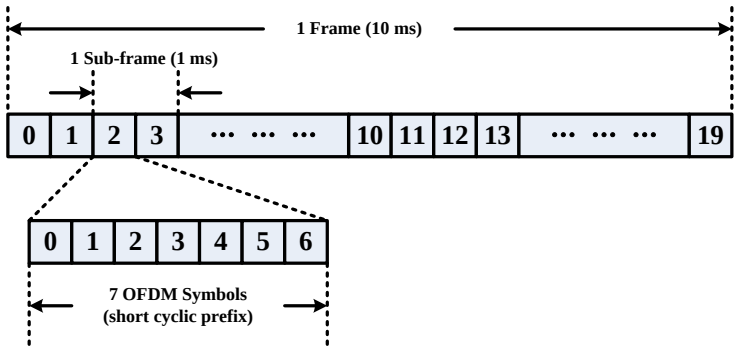

Figure 2.5: *LTE Frame Structure*

transmission can occur simultaneously during each frame using different carriers. In TDD operation, uplink and downlink are separated in time, but both of them share the same carrier. The guard time in the special subframe is used to provide the necessary guard time for downlink-to-uplink switching.

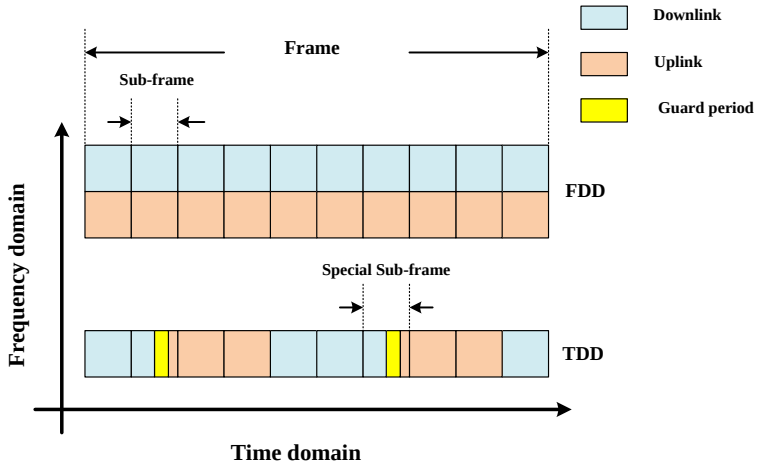

Figure 2.6: *Downlink and Uplink Structure in case of TDD or FDD*

The 3GPP specifications for LTE includes fourteen frequency bands for FDD as shown in Table 2.4 [27].

2.2.4 OFDMA & SC-FDMA

The physical layer of LTE utilizes OFDM as the multi-carrier transmission technology (see Figure 2.7), which creates very narrow band channels by a lot of

Band	Uplink range (MHz)	Downlink range (MHz)
1	1920 – 1980	2110 – 2170
2	1850 – 1910	1930 – 1990
3	1710 – 1785	1805 – 1880
4	1710 – 1755	2110 – 2155
5	824 – 849	869 – 894
6	830 – 840	875 – 885
7	2500 – 2570	2620 – 2690
8	880 – 915	925 – 960
8	1749.9 – 1784.9	1844.9 – 1879.9
10	1710 – 1770	2110 – 2170
11	1427.9 – 1452.9	1475.9 – 1500.9
12	698 – 716	728 – 746
13	777 – 787	746 – 756
14	788 – 798	758 – 768

Table 2.4: *Paired frequency bands defined by 3GPP for LTE*

sub-carriers that are orthogonal to each other. It can be used as a general digital modulation scheme that all the OFDM sub-carriers are utilized for transmission for a single transmitter to a single receiver. Moreover, as OFDM allows for time-separated and simultaneous frequency-separated transmissions to/from users, it is also considered as a multiple access scheme – Orthogonal Frequency Division Multiple Access (OFDMA). In LTE, OFDMA is used in downlink phase. However, due to the importance of low-power mobile terminal, Single-carrier Frequency Division Multiple Access (SC-FDMA) is selected as the multi-carrier transmission scheme for uplink (see Figure 2.8) [28]. One major difference between OFDMA and SC-FDMA is that SC-FDMA requires subcarriers assignment to the users to be adjacent for each time instance, but OFDMA does not have this restriction.

2.2.5 Scheduling & CQI

The function of scheduler in Base Station (BS) is to determine to/from which MS to transmit/receive data as well as on which set of RBs. The MS only follows the scheduling commands from its serving cell. The ICI coordination between different BSs is dependent on signaling over the X2 interface. The scheduler also controls the selection of transport block size, modulation scheme and coding rate. The logical channel multiplexing is controlled by eNB in the downlink, but by MS in

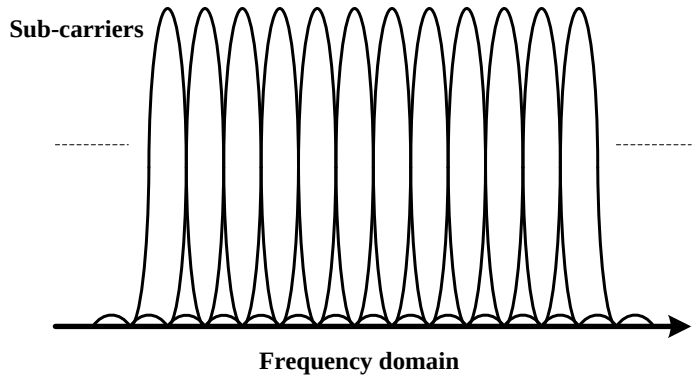

Figure 2.7: *OFDM Orthogonality*

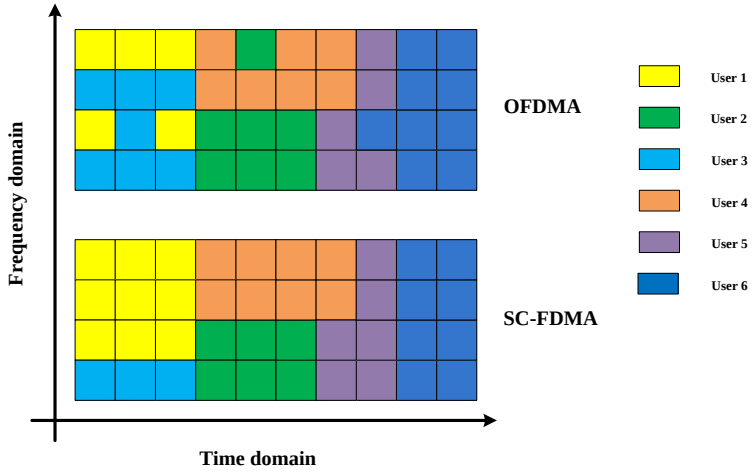

Figure 2.8: *OFDMA and SC-FDMA*

the uplink.

A key feature of LTE downlink is channel-dependent scheduling, which is supported by channel-status report from MS. The main channel-status report provided by MS is Channel Quality Indication (CQI) [29] [30], which recommends the modulation scheme and coding rate for the downlink transmission using a certain set of consecutive RBs. According to the channel-status report, the scheduler can exploit the multi-user diversity gain by performing dynamic resource allocation.

2.3 Genetic algorithm

Genetic Algorithm (GA) is a branch of evolutionary algorithms, which generates solutions to optimization problems or searching problems by evolution, such as inheritance, crossover, mutation and selection [31]. Generally, GA can be employed as a good optimization tool, if the searching/optimization problem is complex and hard to optimize.

2.3.1 Modeling for GA

In biology, genes are composed of chromosomes, which encodes a trait (e.g. skin color). In genetic algorithm, possible solutions are also represented by chromosomes. Typically, these chromosomes are encoded by binary strings of 1s and 0s. GA starts the evolution from a population of randomly generated individuals towards the better solutions with the applying genetic operators. Generally, there are three most significant aspects that should be done in order to model the optimization problem feasible to applying GA [32]:

- Definition and implementation of chromosomes.
- Definition of the objective function, which is able to evaluate different individuals.
- Definition of the genetic operators.

There are three main operations of GA that play an important role in evolution and determine the performance of GA. The first one is crossover, which is generally defined to use two individuals (parents) to produce two more new individuals (children) as Figure 2.9. The second one is mutation, which represents the errors during copying genes from parents (see Figure 2.10). The third one is selection, which filters the bad solutions and keeps the good ones.

After modeling the problem for GA, it starts the following steps [33]:

(1) Randomly generate some chromosomes for initialization.

(2) Use the defined objective function to evaluate each chromosomes.

(3) Select some chromosomes with good results from objective function as parents.

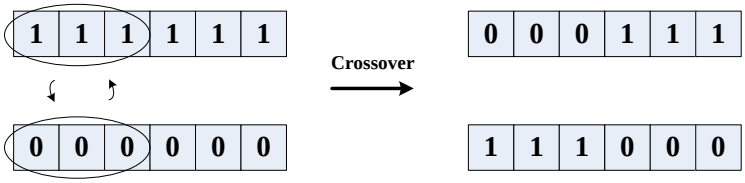

Figure 2.9: *Crossover*

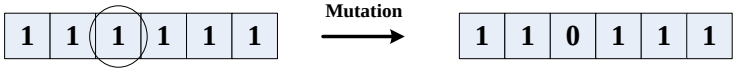

Figure 2.10: *Mutation*

(4) Perform crossover and mutation with a given probability over the parent chromosomes to generate new offsprings

(5) Replace the good chromosomes with the worst ones to create a new population.

(6) If the end condition is not satisfied, then go back to the second step. Otherwise, stop and return the best chromosome.

2.3.2 GA parameters

Usually, the main parameters of GA are: generation number, crossover probability, mutation probability and population size. The generation number decides the number of the generation of chromosomes. Crossover probability and mutation probability decide the probability of crossover and mutation when the parent chromosomes to generate new offsprings. The population size controls the population of chromosomes.

2.3.3 Performance-determinant factors

The GA usually converges and offers a good solution for the optimization problem, if the objective function can distinguish good and bad solutions and the optimization problem has a global optimal solution. Moreover, the convergence speed is dependent on the initialization of the chromosomes, the method of the operators and their parameters' settings. In order to achieve good solution, it is important to use a reasonable large generation number to allow GA to evaluate more possible

solutions. Generally, GA converges with a large enough generation number. The solution provided by GA can then be considered as a good solution.

Chapter 3

Related Work, Scope of the Thesis

3.1 Related work

In [10], the power control coordination between base stations is pointed out and it is considered as a potential method for ICI coordination. Furthermore, schemes such as adaptive FFR with high spectral efficiency which is also the goal of SFR is proposed. Some recent research has been done in order to find better ICI coordination approaches. In [16], a good foundation is provided for the investigation of SFR for ICI coordination of LTE networks. It proves the performance of the interference-limited networks highly depends on the configuration of the power mask which is implemented by SFR. There is a significant performance gap between a smart power mask and a simple one without ICI coordination. [16] is a good theoretical evidence for investigation of SFR, but it neither analyzes the complexity of SFR and nor provides a practical method for SFR.

Some SFR schemes with simple power masks are investigated in [34], [35] and [36]. In [34], the SFR scheme splits cell into a center zone and an edge one. The bandwidth is also divided into two parts, where each part is used in one of the zones. But the power of the bandwidth assignment for the edge zone is higher then that for the center zone. The ICI is controlled by avoiding adjacent cells using high power for the edge zone. Combined with a proposed scheduling algorithm and realistic radio propagation setting, it show the ability of SFR to improve the cell-edge user's performance by shifting the system capacity from cell center users to those at cell edge. In [35], the similar static SFR scheme is also investigated, but it improves and introduces an idea of changing the power allocation factor for cell-

center subband according to the traffic load, although it does not provide how to perform the allocation adaptively. In [36], the power planning for RBs are designed according to the density of users' geometric distribution; the bandwidth is divided into tree parts according to the density of users at cell-center, cell-intermediate and cell-edge area, and then each of the bandwidth gets a different power level. For this scheme, there is no constraint for later coming local scheduling; each cell just performs scheduling by itself with a given power mask. The advantage of this scheme is simplicity and the local scheduler gets its freedom to do RB assignment. It can be easily adaptive to different distribution of users because of the mobility. However, this kind of power allocation is not able to provide how to find a reasonable power and how much power should be used for different RBs. These schemes only use simple static power allocation for ICI coordination and do not need any coordination for local scheduling when assigning RBs.

There are also some papers (see [1], [2], [37] and [38]) which are trying to find a good ICI coordination scheme with a joint static power and RB allocation; there are some constrictions when a RB with high/low power is assigned to a user. In [1], a SFR with a static frequency planning combined with a modified proportional fairness scheduling is provided to exploit frequency selective scheduling gain and larger peak rate for cell edge user. In order to do ICI coordination, the author classifies the users by their geographical locations and distinguishes them by cell edge user and cell center user, see figure 3.1(a). Moreover, different cells have their own power profile planning, see figure 3.1(b). The proposed scheme is designed to modify the scheduling priorities of different types of users in order to make the cell edge users have more probability to use the frequency band with high power and the cell center users have more probability to use frequency with low power. Although this scheme is of low complexity for its decentralized ICI coordination and simple scheduler, it has some drawbacks; it can only adapt to proportional fairness scheduling, and it does not give a way to calculate the priorities and, in addition, the power profile is a static one which may not adapt to all kinds of user distribution and prevent scheduler exploiting more gains. In [2], a joint power and frequency coordination scheme based on frequency sectorization and power masks are proposed for ICI coordination. The frequency sectorization and power masks are designed as figure 3.2; the frequency bandwidth is divided into different subbands according to a given area of the cell and different subbands are assigned with different power level in order to control the ICI. In this scheme, the RB and power allocation are joint to minimize the total power consumption for a specific data rate. In order to guarantee the cell edge user performance, the RB for cell-edge subband will be assigned to the users of high requirements for power consumption. This scheme makes the ICI under control by different power allocations of the same bandwidth among cells and the restriction of the usage of subband according to

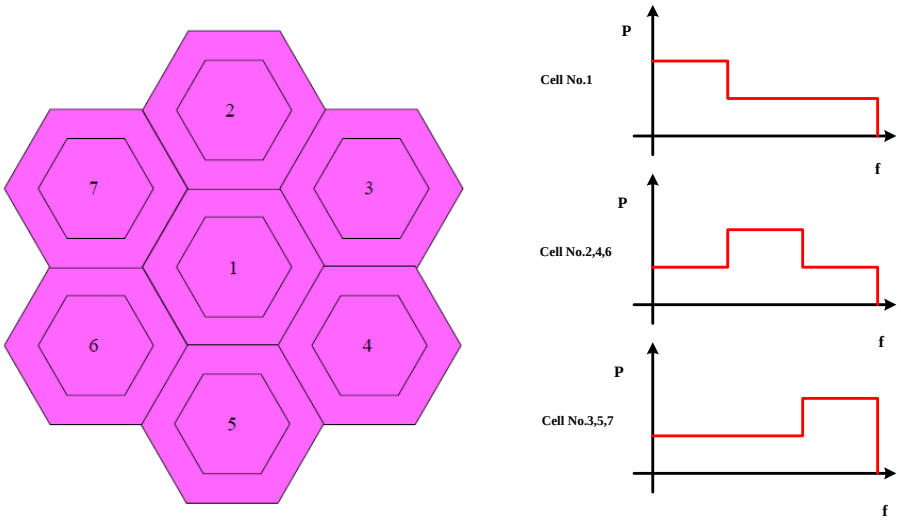

(a) Cell Planning for [1] (b) Power Profile Planning for [1]

Figure 3.1: *Cell and Power Profile Planning for [1]*

the user requirement of transmit power; it uses the subband for cell center user to increase the resource utilization efficiency and uses the subband for cell edge user to compensate the performance loss due to the ICI. This scheme is of low complexity because of decentralized design. However, this scheme has some drawbacks; it does not provide a good way to calculate the power allocation for RBs and uses a static power mask which can not exploit the diversity from ICI coordination according to user distribution. It is also very hard to provide a good way to divide the frequency bandwidth for cell center or cell edge user because of the uncertainty of the traffic load distribution. In [37], a relatively decentralized Adaptive Soft Frequency Reuse (ASFR) scheme by exchanging the interference indicator with neighboring cells for LTE uplink is proposed. This scheme categorizes the terminals into cell-center and cell-edge users and splits the bandwidth into two parts with different reuse factor for the two-type users. The ICI coordination is performed by taking care of RB reuse avoidance. This scheme controls the ICI and improves the spectral efficiency by borrowing idle RBs from neighboring cells and restricting RB reuse. Although borrowing RB from neighboring cells for cell-edge bandwidth is intuitively very appealing, realizing it in practice is no trivial task; it requires each cell to exchange the interference indicator with the others frequently at the expense of using huge amount of over-headers. In addition, this scheme requires scheduler performs the RB allocation only with path loss without information of instantaneous channel gain – fading gain, which prevents the scheduler exploiting channel diversity gain. In [38], an SFR/ASFR scheme for a centralized control system is provided. It

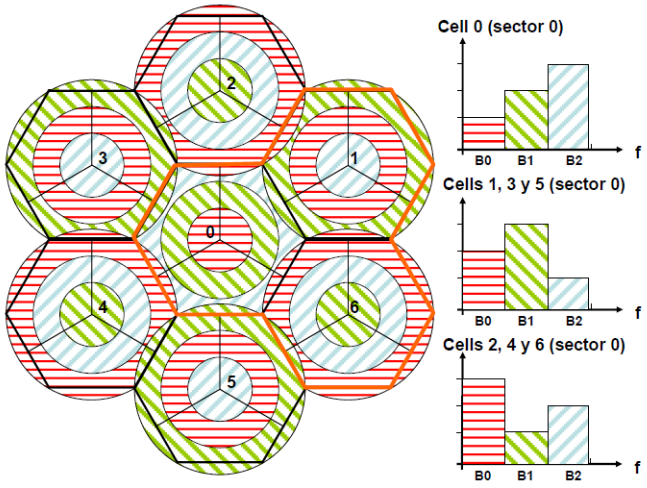

Figure 3.2: *Frequency sectorization and power masks for [2]*

introduces a central controller which collects all the information of coordinated cells and distributes the scheduling information to them, meaning all the resource management optimization problem should be solved by the center controller. In the proposed scheme, the system bandwidth is split into several subbands and cell edge users will be served with the subbands of high transmitted power. The power allocation for ICI coordination is performed to satisfy the spectral efficiency requirement by employing the user's geometric information and it can also be adaptive to the changing of users' geometric distribution. However, the restriction of bandwidth assignment for cell edge user is not able to exploit the frequency diversity gain that the subband with the lower power allocation may have at a certain instant time. In addition, the central controller which receives all the information from its serving cells requires the system of very high complexity and of high expense for exchanging the information, which is very impractical.

The work done in this thesis is to find a ASFR of reasonable system complexity, which can be adaptive to the traffic load and offer the local scheduler freedom to perform RB allocation. The system of the proposed ASFR in section 4.3 is modeled to maximize the user of worse performance among the network. The work done in [39] [40] and [41] serves as the foundation of the optimization problem for the ICI coordination investigation. In addition, the work done by Naghibi and Gross in [42] offers a good approach to describe the distribution of SINR in wireless channel and approximate the average channel capacity for interference-limited system and the model of packet-delay-based local scheduling in section 4.2 is also introduced by them. The simulation environment which is used for performance evaluation has the basic framework created by M. Bohge in TU Berlin and F. Naghibi in KTH.

3.2 Thesis scope

Within this thesis, the investigation mainly focuses on SFR scheme in LTE system. This thesis work only considers ICI coordination approach for LTE downlink phase. Within the scope of this work, ICI coordination and local scheduling are two separated steps. The ICI coordination is achieved by employing good power allocations, and it does not make any decision about RB allocations. After ICI coordination, the scheduler uses scheduling algorithm according to different requirements of Quality of Service (QoS) to assign RBs. This thesis focuses on finding a good ASFR for centralized ICI coordination which can exploit the diversity from different traffic loads and different distribution.

From a link perspective, LTE downlink phase allows for a more flexible analysis if the desired MS location is available. The MS's average channel gain to its associated BS as well as all the potential interfering BSs can be easily determined. Hence, this provides a possible way to estimate the SINR. This thesis employs pre-calculated propagation maps and a position technology (i.e. Global Positioning System (GPS) [43]) to achieve the average channel gain for ICI coordination. In this way, the overhead resulted from transmitting channel status information can be reduced because of no need for terminals to feedback them for ICI coordination. However, employing the GPS means that the positioning deviation is also introduced, which makes the average channel gain to be erroneous.

The current SFR schemes (such as [1], [2]) generally use static power allocation to mitigate ICI. However, since the channel state highly depends on the geographical location of a MS, static SFR can not be efficient if the position is changed. Therefore, in this thesis, investigation is carried out to find an ASFR which overcomes the problem caused by terminal's mobility. Since different types of traffic over the networks have their own QoS requirements, this thesis work only considers to schedule Voice over Internet Protocol (VoIP) traffic. The goal of the thesis is to design a good ASFR scheme that can improve the overall QoS for VoIP calls and evaluate the its performance. Within the scope of thesis, the ICI coordination is modeled to maximize the minimum estimated data rate of the users in the system by a central entity. The execution of ICI coordination is done by the central entity which collects the average channel status of all the users and employs GA to search for the solution of the max-min optimization problem.

Chapter 4

System Model & Design

4.1 System Model Overview

4.1.1 Basic assumptions

The radio resource management in 3GPP LTE involves three dimensions: frequency, time and space. In this report, the RB which spans both frequency and time dimensions is the main resource element to be considered. The Transmission Time Interval (TTI) is defined by the unit of the time dimension span of RB. Within this thesis, the system model will only consider resource allocation for down-link phase and the intra-cell interference is considered to be successfully avoided. Furthermore, VoIP is the only traffic in the system. It is assumed that there are only two BSs, which means there is only one interference source. It should be noted that the TTIs are assumed to be synchronized among cells within the scope of report. For the simplicity, the theoretical Shannon capacity of a channel is used for measuring the throughput.

4.1.2 System model description

Physical layer model

The system is a OFDM network with a total frequency bandwidth B Hz at a center frequency f_c Hz. The bandwidth is split into N sub-carriers each of which has a

frequency spacing $\triangle f = B/N$ and symbol length $T_s = 1/\triangle f$. The maximum transmit power for downlink phase is P_{max} and is split among sub-carriers. It is assumed that all the N subcarrier symbols are transmitted simultaneously as an OFDM symbol. Considering the inter-symbol interference, a cyclic prefix of length T_g is added to each OFDM symbol. For each terminal j, the subcarrier n has a channel gain $g^t_{j,n}$ which varies over time and frequency domain. It is assumed that a terminal's channel gain of a group of subcarrier stays constant for the duration of one down-link phase (t) but varies over longer time spans.

Medium access layer model

In downlink, OFDMA is considered as the data multiplexing scheme. N_{RB} adjacent sub-carriers with K OFDM symbols compose the spectral resource unit of LTE system (see Section 2.2.3). RB is the scheduling unit. During the resource assignment, the scheduler performs the power and RB allocation for each cell based on the knowledge of the channel status. Channel quality differences among the sub-carriers belonging to a single RB are negligible, which means each RB is assumed to experience flat fading. According to different requirement of QoS, the scheduler can have different scheduling goal for resource allocation.

Centralized multi-cell scheduling system

This section provides a system model (see Figure 4.1) for multi-cell OFDMA-based cellular network, which mainly handles the packet scheduling and ICI coordination for down-link phase. The procedure of the whole scheduling is as following: when the MSs' packets come and start queuing, the model separates the scheduling into two parts:

- local scheduling: a BS performs local scheduling independently with a given power allocation for each RB. Since VoIP service is delay sensitive, the overall throughput is not the main target when BSs transmit. Therefore, the local scheduler needs to perform packet delay based scheduling, assigning RBs to MSs according to the packets' delays in each down-link phase. The local scheduler at BS does not consider to mitigate the ICI, when it allocates resources and exploits the channel diversity gain. In this way, a further step should handle the ICI problem.

- ICI coordination: In the previous step, it is known that BS will obtain the power allocation from somewhere else. The power adjustment here can be considered as an opportunity to perform ICI coordination. Thus, a central entity which can communicate with all the BSs is introduced in the network and performs power adjustment for all RBs among a group of cells. Since communications between central entity and BSs are expensive and it is difficult to provide all the instantaneous scheduling information (such as each RB channel status of each MS) for central entity within every TTI, it is better for the central entity to use limited information for power adjustment either from the complexity or expense point of view. Within this thesis, the ICI coordination is performed only with the average channel gain which is mainly dominated by MS position. In this way, the power allocation needs to be updated according to the changing of average channel gain because of MS's mobility. Therefore, the ICI coordination approach is an kind of adaptive soft frequency reuse schemes.

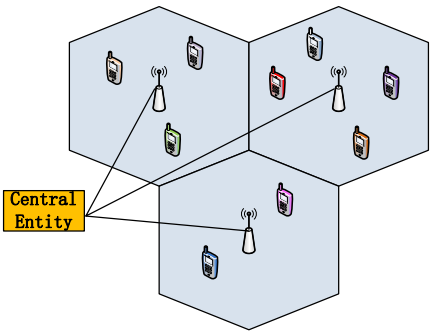

Figure 4.1: *Centralized multi-cell scheduling system*

In short, the central entity controls the ICI by coordinating the power adjustments for BSs within each period, and the BSs receive and update the power masks for their frequency bands and conduct the local scheduling.

Overall scheduling goal

Since VoIP is the only traffic to be considered, the overall scheduling goal is to support as many traffic load as possible for down-link phase.

4.2 Local Scheduling

4.2.1 Packet delay based local scheduling

In the previous Section 4.1, the framework of the centralized multi-cell system is provided. This section will mainly focus on the details of the local scheduling part. Within this section, it should be made clear what problem should be handled with if it is the delay-sensitive scheduling, and a solution model needs to be figured out.

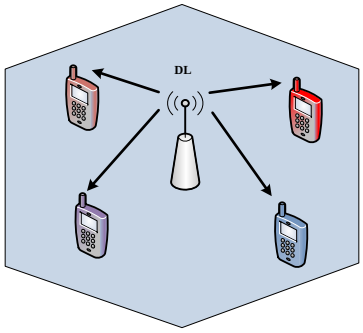

Figure 4.2: *Single cell multi-user system*

In this section, a single-cell multi-user OFDMA system (see Figure 4.2) is to be considered. As it can be seen in Figure 4.3, the BS has a queue, which contain some packets to be transmitted to different MSs in the down-link phase and the local scheduler will decide which packet should be transmitted during the next down-link phase. The left unscheduled packets start queuing and wait to be scheduled in the next period. Therefore, it is obvious that the QoS is dependent on the performance of local scheduling scheme. In order to keep the overall low packet delays in all the queues and improve the QoS,there is a need for a good packet delay based scheduling scheme.

4.2.2 Problem statements and FIFO

Packet delay based scheduling scheme actually is a kind of optimization problems, which aims at minimizing the overall packet delays in a cell. In this section, it is assumed that the scheduler should try to schedule the packets of larger delays with a higher priority than those of smaller delays.

Moreover, it should be aware that there are some information the scheduler can

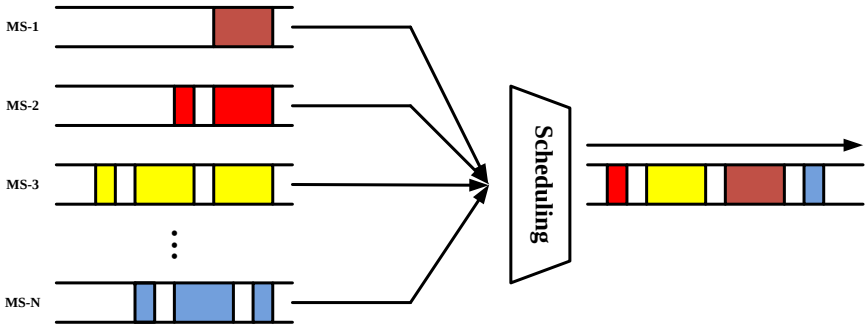

Figure 4.3: *Packet delay based local scheduling*

use for local scheduling:

- It has pre-determined power allocations, denoted as power mask, for each RB. As it was mentioned in system model, the local scheduler only uses this power mask directly and how to obtain a good power mask is not the its duty. It is the central entity that takes care of calculating the power mask.
- It uses CQI feedbacks from its served MSs to assist the scheduling. Each MS sends CQI feedbacks which contains SINR of each RB back to BS. In this way, the local scheduler has the information of estimation for the next instantaneous channel states. Therefore, the capacity $C^t_{j,n}$ of each RB n for MS j at time instant t is available for the scheduler, providing a possibility to exploit the channel diversity.
- In order to perform packet delay based scheduling, the local scheduler also need the queuing states – packet delay and packet size. Each packet q that belongs MS j at time instant t has a stamp showing its delay $d^t_{j,q}$ as well as packet size $S^t_{j,q}$ and the scheduler updates with its queuing states before it starts scheduling.

First In First Out (FIFO)

Since the local scheduling scheme is not the main work of the thesis, here the simplest scheduling scheme – FIFO – is applied for the packet delay based scheduling. The basic idea of FIFO scheduling for LTE system is to transmit the packet of the largest delay with the highest priority. In order to perform FIFO, the scheduler needs to do the following things (for details, see local scheduling implementation in Chapter 5):

- All the packets that arrive at the BS should be ordered in a descending order according to their packet delay. The packet with the largest delay will be scheduled first. If packets have the same delay, then order randomly.
- Scheduler creates a preferred RB list for each MS when it allocates RB for MS to transmit packets. The scheduler collects the CQI feedbacks of each RB from each MS and creates the preferred RB list with a descending order of each RB's capacity. If RBs have the same capacity, then order them randomly.
- When a MS's packet needs to be transmitted, the scheduler assigns the available RB on the top of the MS's preferred RB list. The total assigned RBs' capacity should be sufficient for the transmission of the packet. If the a RB is assigned, it should be removed out from all the MSs' preferred RB list.
- The scheduler stops the RB assignment until the unassigned packet with the largest delay can't be transmitted or there is no idle RB left.

Since the BS uses an assigned power allocation which decides the capacity and ICI of each RB, it is the key point that ICI coordination affects the local scheduling performance. Therefore, it may be possible that there is an approach to improve the system performance with a good power allocation. It is to be investigated in the next section.

4.3 Inter-cell Interference Coordination

In Section 4.2, the problem of local scheduling has been addressed, and a scheduling approach has been provided. This section mainly investigates the ICI coordination problem which has not been solved by local scheduler. In this thesis, the ICI coordination is isolated from the local scheduling; it keeps the proposed system model compatible with the general system and makes system update easy. In this section, it aims at finding a realistic approach of low complexity for ICI coordination.

4.3.1 Centralized multi-cell scheduling - power adjustment

The proposed centralized scheduling approach consists of the following steps: 1.) the central entity derives the average channel gain of each MS from the position technology and propagation maps; 2.) then it adjusts the power allocation of each RB in each cell. Although the power masks are provided by central entity, the RB and packets assignments are decided by local schedulers; it offers the possibility of exploiting the dynamic channel gain, and to some extent, compensates the disadvantage of using less accurate channel estimation – average channel gain. Since the average channel gain is dependent on the position of MSs which does not change very fast, therefore, the central entity only needs to update the power allocation in a large time scale (e.g. 10 superframes [1]). Moreover, ICI coordination at central entity has to solve a non-linear optimization problem which is of high computation expense.

Problem statements and formulations

Before formulating the scheduling problem at central entity, let's first describe the problems that central entity should deal with. Considering the complexity, the central entity only uses limited information for power adjustment:

- information of average channel gain from the position technology and propagation maps,
- no feedback from MSs with instantaneous channel property,
- no RB allocation and queuing state information from BSs.

[1] Superframe is a LTE terminology which represents 10 1ms-duration frames

In this way, the central entity considers each VoIP service has a minimum rate requirement. It is known in Section (4.1) that the overall scheduling goal is to maximize the supported traffic load. Hence, in this section, the scheduling goal of central entity is formulated to maximize the minimum estimated achievable rate in the system. So it is modeled as a max-min optimization problem [39] [40] [41] based on the average channel gains to find the power allocation of each RB for every cell. The power assignment $l_{n,k}$ of RB n in cell k and the assignment $a_{j,n,k}$ of RB n for MS j in cell k are the variables of the assignment problem. However, the RB assignment $a_{j,n,k}$ and the power allocation $l_{n,k}$ are both linear-relaxed. Relaxing the RB assignment is because a RB can be assigned to different MSs within a large long time scale (10 superframes), although it can only be assigned once within a TTI. The formulation is as below:

$$\max_{A,L} \quad r, \tag{4.1}$$

$$s.t. \quad \sum_{n} a_{j,n,k} \cdot C_{j,n,k} \geq r, \ \forall j,k, \tag{4.2}$$

$$\sum_{j} a_{j,n,k} \leq 1, \ \forall n,k, \tag{4.3}$$

$$\sum_{n} l_{n,k} \quad \leq P_{max}, \ \forall k, \tag{4.4}$$

in which, r is the minimum estimated achievable data rate among all the MSs in the system, which should be maximized. Constraint (4.2) calculates the estimated rate for an MS j in cell k according to the assumed the RB assignment $a_{j,n,k}$ as well as the average capacity $C_{j,n,k}$ of the corresponding RB n which is assigned to an MS j and finds the minimum estimated rate among all the MSs. The average capacity $C_{j,n,k}$ will be discussed later and $\gamma_{j,n,k}$ is the instantaneous SINR of RB n assigned to MS j in cell k as below [16]:

$$\gamma_{j,n,k} = \frac{l_{n,k} \cdot h^2_{j,n,k}}{\sum_{k' \neq k} l_{n,k'} \cdot h^2_{j,n,k'} + N_{\mathrm{o}} \cdot B_n} \tag{4.5}$$

in which N_{o} is the noise power density (here noise is considered Gaussian) and B_n is the bandwidth of RB n.

Constraint (4.3) guarantees the assignment of each RB should not be more than 1 which controls a RB total assignment amount. The last constraint (4.4) limits the power consumption $l_{n,k}$ of each RB not exceeding the total available power in cell k. Note this optimization problem is proven to be NP-complete [44].

Since the central entity has no feedback about the RB assignments from BSs, in order to estimate the data rate, the central entity assumes RBs to be assigned

to MSs. However these RBs assignment prediction will not be used. It is only a prediction that helps to search for a good power adjustment. The local scheduler still has its freedom to assign RBs as well as the packets. Therefore, the output of the model in this section has RB assignment and power allocation, but only the latter one is used further.

4.3.2 Channel capacity estimation

In Equation (4.2), the ICI coordination is also dependent on the average capacity of each MS's RBs. The upcoming LTE is an interference-limited system. In order to predict the channel capacity and assist central entity to perform ICI mitigation, there should be a good approach to estimate channel capacity for dynamic resource allocation in the interference-limited OFDM system.

Since the central entity has the prediction of RB assignment and the power allocation, then it is possible to predict the instantaneous SINR. Then as the noise is assumed to be Gaussian, the Shannon theory can be used for channel capacity estimation. From the Shannon theory, it is known that the instantaneous channel capacity is dependent on the instantaneous SINR. From Equation (4.5), the most difficult thing is to achieve the instantaneous channel gain of the desired signal or the interference signal, $h^2_{j,n,k}$ or $h^2_{j,n,k'}$. These two different types of channel gain are independent random variables. Since there is no related direct feedback for these channel gains and the only available information is average channel gain from propagation maps, there are several ways to model this problem.

In this section, three different approaches are provided which are adaptive to two-cell scenario. The average capacity is derived based on an arbitrarily chosen RB by an MS in a cell.

Naive capacity estimation

The first approach is called naive capacity estimation in this section, which is the general way. The capacity is estimated without instantaneous channel gain, but only with average channel gain. The average capacity function $C_{j,n,k}$ is rewritten as following:

$$C_{j,n,k} \approx B_n \cdot \log_2(1 + \frac{P_S}{P_I + N_0 \cdot B_n}), \tag{4.6}$$

where $P_S = l_{n,k} \cdot \overline{h}^2_{j,k}$ is the received signal power, $P_I = \sum_{k' \neq k} l_{n,k'} \cdot \overline{h}^2_{j,k'}$ is the received interference power, and $\overline{h}^2_{j,k}$ or $\overline{h}^2_{j,k'}$ is the average channel gain; the average channel gain replaces the instantaneous channel gain in equation (4.5). However, for two-cell scenario, the way to find the average capacity of two independent random variables ($h^2_{j,k}$ and $h^2_{j,k'}$) is not as simple as that in Equation (4.6) by replacing the instantaneous channel with the average channel.

Static RB allocation capacity estimation

In order to achieve a good estimation of channel capacity, the Rayleigh fading channel model is taken into account. Research has been carried out to merge two random variables into one and find the distribution of the SINR in [42]. Here, the probability density function $P(\gamma_{j,n,k})$ of the SINR per RB is rewritten as below:

$$P(\gamma_{j,n,k}) = [\frac{N_0 \cdot B_n}{P_I \cdot \gamma_{j,n,k} + P_S} + \frac{P_S \cdot P_I}{(P_I \cdot \gamma_{j,n,k} + P_S)^2}] \cdot e^{-\frac{N_0 \cdot B}{P_S} \cdot \gamma_{j,n,k}}, \ k \neq k'. \tag{4.7}$$

Then, the average capacity of a RB is derived as the following:

$$\begin{aligned} C_{j,n,k} \approx B_n \cdot \int_0^{+\infty} & [\frac{N_0 \cdot B_n}{P_I \cdot \gamma_{j,n,k} + P_S} + \frac{P_S \cdot P_I}{(P_I \cdot \gamma_{j,n,k} + P_S)^2}] \\ & \cdot e^{-\frac{N_0 \cdot B_n}{P_S} \cdot \gamma_{j,n,k}} \cdot \log_2(1 + \gamma_{j,n,k}) \ d\gamma_{j,n,k}, \ k \neq k', \end{aligned} \tag{4.8}$$

where $P_S = l_{n,k} \cdot \overline{h}^2_{j,k}, P_I = \sum_{k' \neq k} l_{n,k'} \cdot \overline{h}^2_{j,k'}$, and $\overline{h}^2_{j,k}$ or $\overline{h}^2_{j,k'}$ is the average channel gain.

Equation (4.8) is called static capacity estimation through the whole thesis. This is because the central entity assumes each MS gets an static assignment of RBs, which means the RBs assignment is fixed and no channel diversity is taken into account.

Dynamic RB allocation capacity estimation

Since the local scheduler exploits the channel diversity, the best way is to have an approach to estimate the channel capacity with considering dynamic RB allocation.

A similar approach has been taken in [42]. The probability density function of the SINR per RB is rewritten as below:

$$\begin{aligned} P(\gamma_{j,n,k}) =& A_j[1 - \frac{P_S}{P_I \cdot \gamma_{j,n,k} + P_S} \cdot e^{-\frac{N_0 \cdot B_n}{P_S} \cdot \gamma_{j,n,k}}]^{A_j - 1} \\ & [\frac{N_0 \cdot B_n}{P_I \cdot \gamma_{j,n,k} + P_S} + \frac{P_S \cdot P_I}{(P_I \cdot \gamma_{j,n,k} + P_S)^2}] \\ & \cdot e^{-\frac{N_0 \cdot B_n}{P_S} \cdot \gamma_{j,n,k}}, \ k \neq k', \end{aligned} \tag{4.9}$$

Then the RB's average capacity can be achieve from the probability density function:

$$\begin{aligned} C_{j,n,k} \approx B_n \cdot \int_0^{+\infty} & A_j[1 - \frac{P_S}{P_I \cdot \gamma_{j,n,k} + P_S} \cdot e^{-\frac{N_0 \cdot B_n}{P_S} \cdot \gamma_{j,n,k}}]^{A_j - 1} \\ & [\frac{N_0 \cdot B_n}{P_I \cdot \gamma_{j,n,k} + P_S} + \frac{P_S \cdot P_I}{(P_I \cdot \gamma_{j,n,k} + P_S)^2}] \\ & \cdot e^{-\frac{N_0 \cdot B_n}{P_S} \cdot \gamma_{j,n,k}} \cdot \log_2(1 + \gamma_{j,n,k}) \ d\gamma_{j,n,k}, \ k \neq k' \end{aligned} \tag{4.10}$$

in which, A_j is remaining number of RBs after previous allocation. Here it is assumed that, for a fixed amount of RBs, the local scheduler starts with an MS j and assigns it with a corresponding best RB out of the remaining RBs. Note that here the best does not simply represent the RB of the highest SINR; it represents the most suitable RB or any definition for the "best" according to the scheduling scheme.

4.3.3 Employing genetic algorithm for inter-cell interference mitigation

In previous investigation, the problem formulated for the ICI coordination (equations 4.1 to 4.4) is a non-linear optimization problem which is of very high computational expense and whose global optimization is impractical. Therefore, considering the fact that the central entity has only limited time to find good power masks for ICI mitigation, it is significant to employ an efficient and fast method. In this section, GA is to be employed.

From equations (4.1) to (4.4), it is known that GA should provide the RB assignments and power assignments as the solution of the non-linear optimization. Then, the chromosomes of GA are RB assignments and power assignments, which should evolves toward better solutions. As a general application of GA, these chromosomes perform crossover and mutation to generate the next generation population of solutions. Since the problem formulation introduces some constraints (equations 4.3 to 4.4), some corrections should be done to modify all the new generations to satisfy these constraints. Then, all the chromosomes' performance are measured by a fitness function (the minimum data rate among the whole served MSs). Those of larger minimum data rate are selected as the parents of the next generation, and the rest of chromosomes are filtered out by the fitness function. After the selection, these selected chromosomes again perform crossover and mutation. All above processes (crossover, mutation, correction and selection) repeat until the time limited is reached or a good solution is found (GA converges).

Moreover, because a good initialization of GA can increase the GA convergence speed, leading to finding a sub-optimal solution quickly. So it is helpful to have a good way to initialize the chromosomes, when the central entity starts to run GA. The average channel gain is dependent on the position of a MS and the average channel gains of close positions are highly correlated. As the MS's position is hardly changed within a small number of TTIs, the solutions of previous ICI coordination can be used to initialize the current run of GA.

4.3.4 Ray tracing, positioning technology and propagation maps

From Section 4.1, it is known that the central entity is responsible for ICI coordination and it performs an centralized scheduling; this also indicates central entity should communicate with BSs. From the global optimization point of view, the central entity should have the CQI feedbacks from all the MSs in the networks. However, this is unrealistic and it would consume a lot of resources, even if the transmission delay were not considered. Therefore, in this thesis, a position technology and a propagation map are applied to assist the estimation of channel states based on ray tracing.

Ray tracing

Generally, the variation due to shadowing and the effect of path loss are modeled as following:

$$\alpha[dB] = \alpha_{\mathrm{PL}}[dB] + \alpha_{\mathrm{SH}}[\mathrm{dB}]. \tag{4.11}$$

There is also another approach based on ray theory to measure this combined effect; this propagation method considers a number of rays can be traced from a given transmitter location to a known receiver location, use the electrical lengths of the various ray paths to calculate the amplitudes and phases of the component waves and then calculate the signal strength. In addition, the changes in amplitudes and phases resulted from propagation through and reflection from obstacles along the ray path can be found in [45] [46].

Therefore, the combined effect of path loss and shadowing can be measured by the ray tracing algorithm based on the photon mapping from the computer graphics, which provides the geographical information. In this thesis, propagation map method is achieved based on this idea.

Position technology and propagation maps

The position technology, such as GPS, locates a MS's position and the propagation map records the received average channel gain of the signal that is transmitted from the BS. The instantaneous channel gain is replaced with the average channel gain which is mainly dominated by pathloss and static shadowing gain. In this way, although the pathloss and shadowing are available, no information about the fading is given. The central entity only collects all the location of MSs in the networks to reduce the consuming of resources at the expense of losing the accuracy of the channel estimation. In figure (4.4), the average channel gain (2 meters above the ground surface) of two BSs in downtown Aachen is shown.

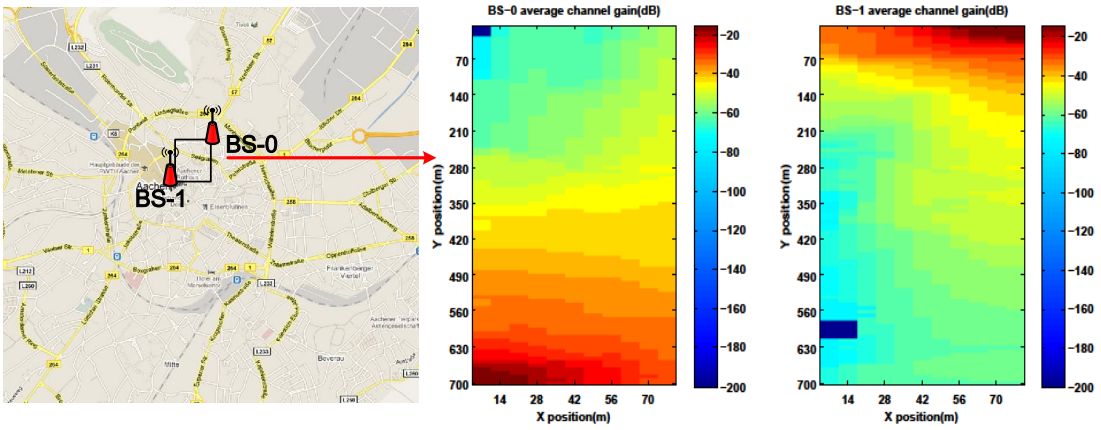

Figure 4.4: *Propagation maps of the chosen area of Downtown Aachen. X, Y are geographical coordinates. It shows the received signal average gain at 2 meters above the ground surface.*

Chapter 5

Performance Evaluation Methodology

5.1 OMNeT++

OMNeT++ is an object-oriented modular discrete event network simulator. It can be used for traffic modeling of telecommunication networks, protocol modeling, queuing systems as well as other systems in which the discrete event exits. An OMNeT++ model is composed of hierarchically nested modules (see figure 5.1). Those modules at different levels communicate through transmitting messages. A model structure is established by OMNeT++'s NEtwork Description (NED) language. The user implements the function of the lowest level – simple module – with C++ language.

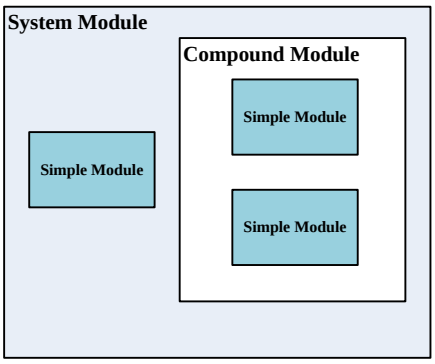

Figure 5.1: *OMNeT++ module structure*

5.2 LTE model in OMNeT++

After the previous work, a LTE system is necessary for performance evaluation. It is obvious that the investigation performed in this thesis is about the end-to-end QoS. As scheduling is one function of eNB in LTE system [1] [47] and VoIP is the only service to be scheduled, in order to avoid simulating the whole LTE system to evaluate the performance of the proposed scheduling scheme, the LTE system is abstracted as some models in OMNeT++ (see figure 5.2); it mainly simulates the dynamic resources allocation of resources and processing the packets from the upper level for downlink. There is no EPC entity implemented; instead it is replaced by a traffic generator module which generates the VoIP packets.

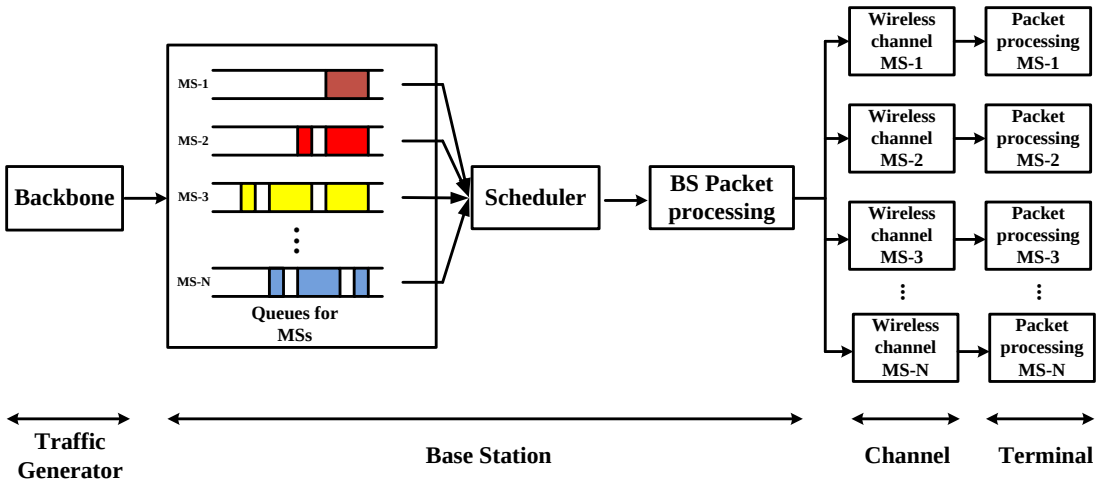

Figure 5.2: *LTE downlink framework in OMNeT++*

5.2.1 Structure of the LTE simulation model

The OMNeT++ LTE model consists of five main modules:

- Traffic generator: creates the VoIP packets and passes them to the base station module.
- Base station: is composed of five submodules – traffic classifier, queues, queue selector, scheduler and packet processor.

[1] eNB: is the only entity of the E-UTRAN that supports all the functions in a typical radio network such as radio bearer control, mobility management, admission control and scheduling.

  - Traffic classifier: distinguishes different types of traffic and passes the packets to corresponding queues.
  - Queues: receive the packets forwarded by the traffic classifier, buffer them, send out the queuing state messages and wait for the dequeue messages. After receiving the dequeue messages from the packet processor, it sends the packets to packet processor. There are different kinds of queues that buffer the packets of different QoS requirements.
  - Queue selector: forwards the queuing state messages to the scheduler, distinguishes different dequeue messages and passes them to the corresponding queues.
  - Scheduler: collects the channel state information from MSs as well as the queuing state information from queues, performs dynamic resource allocation and send scheduling decisions to packet processor. Moreover, it also sends the resource allocation information to the channel generator to update the channel state.
  - Packet processor: receives the scheduling decisions from scheduler and sends out the dequeue messages to queue selector which forwards the messages to queues. After receiving the packets from the queues, it encapsulates the packets with headers and sends them to the corresponding MSs.

- Channel generator: receives the RB allocation from schedulers, the power allocation from the central entity as well as the MSs' positions, and then generates the channel states for corresponding MSs. Afterwards, it sends the channel state information to MSs.
- MS: receives the packets transmitted from the BS, and forwards the channel state information to scheduler at the BS to assist the next scheduling.
- Center entity: receives MSs' positions from the BSs and performs the power adjustment and sends the power allocation to BSs.

5.3 Own implementations

Most of my implementations are located at base station module, mobile station module, channel generator module and central entity module. In the base station module, the work deals with the packet scheduling algorithm and the queuing system – some NED and C++ mixed programmings for scheduling algorithm,

C++ programing for communication between OMNeT++ modules and packet queuing as well as dequeuing. In the channel generator module, the work is mainly about integrating the propagation maps with LTE simulator for the channel state calculation. In central entity module, the work is mainly related with employing GA for ICI coordination and the erroneous channel model. In MS module, the work is mainly about creating MS's mobility models.

5.3.1 Local scheduling implementation

The FIFO scheduler is chosen as the local scheduler. There are two main tasks of scheduler implementation, which are dequeuing and dropping the packets with large delay and RB assignment, see Figure (5.3) and (5.4). Since it is VoIP

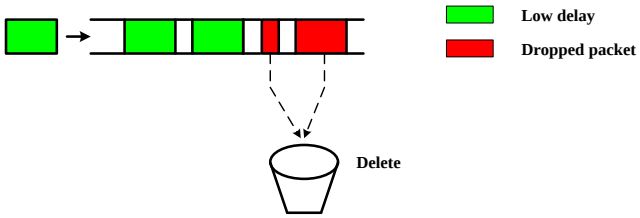

Figure 5.3: *Dequeuing and dropping packets of large delay*

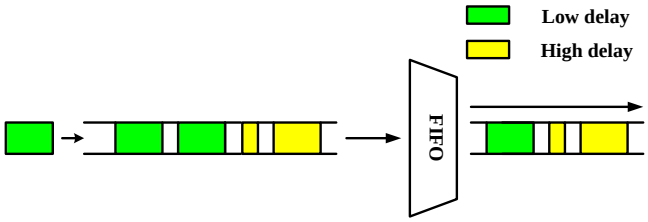

Figure 5.4: *FIFO scheduling*

traffic, a packet with very large delay is meaningless for transmission. It is good for scheduler to delete this kind of packet instead of transmission in order to save the spectral resource. Therefore, it is important for the local scheduler to sort the packets according to their delays and drop those of large delay.

In order to do the scheduling work, the scheduler needs some scheduling information: queuing status, CQI from its serving MSs and power allocation from central entity. Therefore, after scheduler updates the information, it goes to FIFO scheduling scheme, see 5.5(a). Then the scheduler only starts to assign the best

available RB to the packet with the largest delay in the queue until the capacity is enough for transmission or there is no available RB left 5.5(b). The scheduler should guarantee a RB is assigned to a unique MS to avoid intra-cell interference.

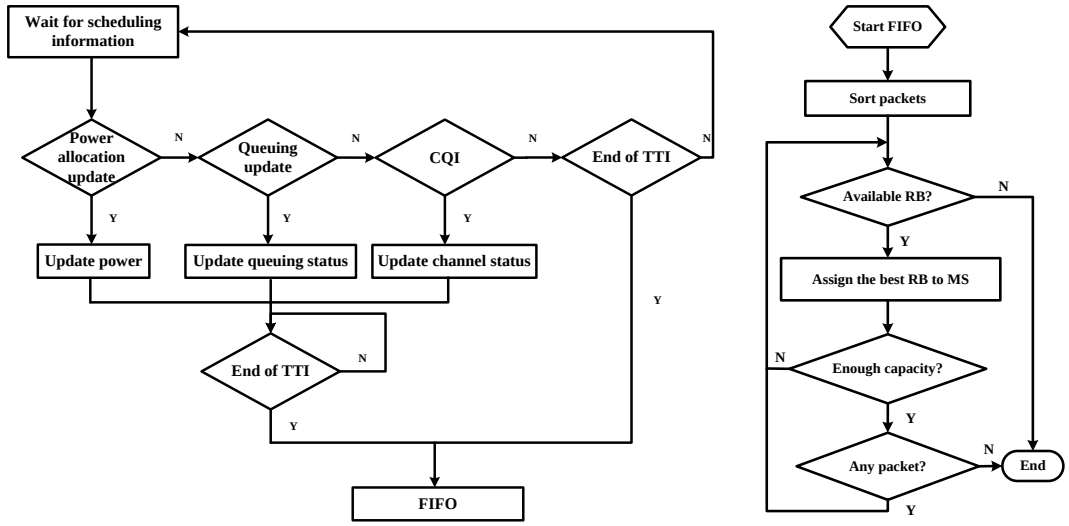

(a) Update scheduling information (b) FIFO implementation

Figure 5.5: *Local scheduling implementation*

5.3.2 ICI coordination implementation

The implementation of ICI coordination includes two parts: employing propagation maps and GA. In order to employ propagation maps, the channel model should be changed to use average channel gain from the maps according to the position of MS instead of using general path loss and shadowing model. In order to solve the ICI coordination optimization problem, the center entity should be implemented with GA.

Before GA gets executed, central entity needs to update all the MSs' positions in the system. Then it uses the position information with the propagation maps to obtain the average channel gain to estimate the channel capacity for GA. Then initialize the variables – power and RB assignments of GA and execute GA. Afterwards, GA performs crossover, mutation, selection, correction, evaluation and selection iteratively until the generation number is reached. Then the central entity output the power mask and send to base stations, see Figure 5.6.

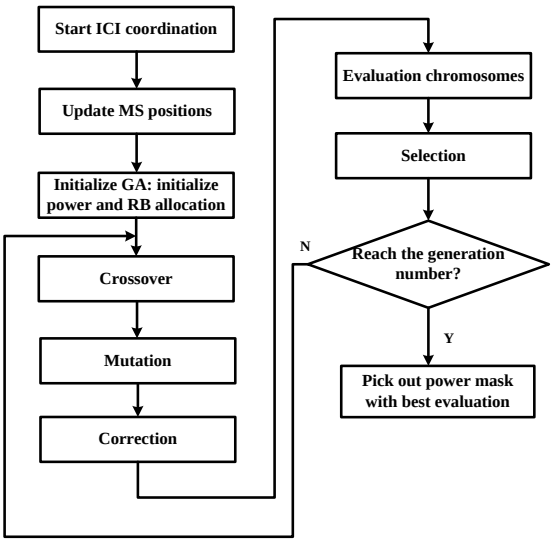

Figure 5.6: *ICI coordination implementation*

5.3.3 Erroneous channel implementation

In order to simulate the error introduced by GPS, there is a erroneous channel model at central entity that simulates the deviation of average channel gain. Then the GA at central entity uses the erroneous channel gain for ICI coordination. In the propagation maps, each pixel represents $7.14696 \times 6.79237m^2$ in the realistic space. The implementation of the erroneous channel model is as following: the erroneous average channel gain of a pixel A is the average gain of the sum of itself and its surrounding pixels, see Figure 5.7.

5.3.4 MS mobility implementation

The implementation of MS mobility is for initialization of a MS position and updating its position. The update message should be sent by this model to scheduler, central entity and channel model for MS mobility. In this thesis, the mobility model restricts MSs not moving out to the neighboring cell, which means there is no handover. The framework of the mobility entity is shown in Figure 5.8.

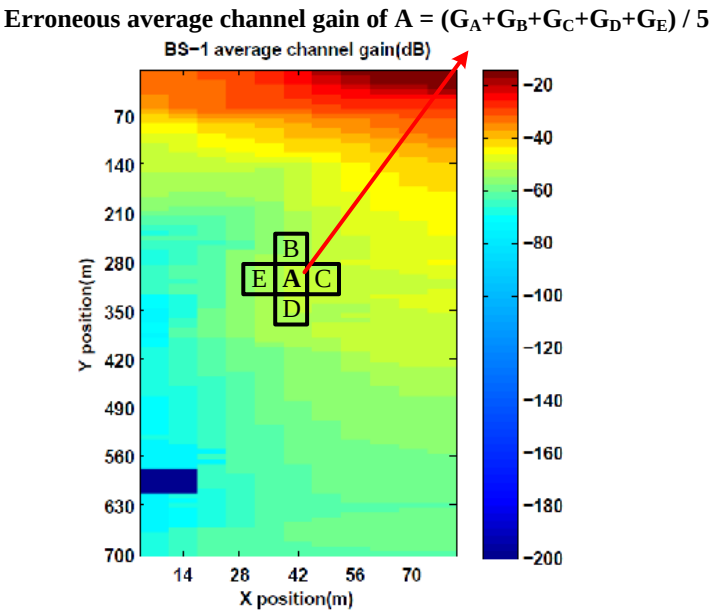

Figure 5.7: *Erroneous channel implementation*

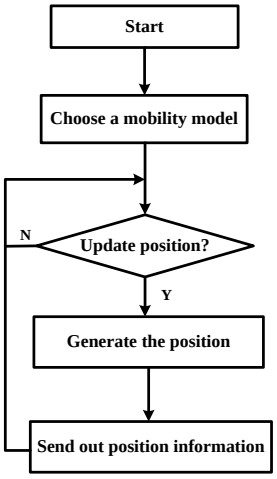

Figure 5.8: *MS mobility implementation*

Chapter 6

Evaluation Scenarios and Results

6.1 Goal of the study

The goal of the investigation is to evaluate the proposed ICI coordination scheme's performance. In this section, a good evaluation approach should be provided in order to show if the ICI mitigation works and how much improvement it offers compared with some prevalent schemes.

6.2 Metrics

Since VoIP service is delay sensitive, a VoIP packet with intolerable large delay in the queue is allowed to be dropped. Before going to further step, it is good to see why a VoIP packet gets dropped. In Figure 6.1, there are a number of VoIP packets coming into the queue and waiting to be transmitted. It is obvious that if the packet arrival speed is larger than the scheduler's serving speed, then the VoIP packet will queue in the buffer and the packet delay will increase. Then those packets with intolerable large delay again block later coming packets to be transmitted with a tolerable delay, resulting in increasing all the packets' delay. From the user experience point of view, it is also not desirable to hear a voice with very long delay. Therefore, it is not a drawback to drop those packets with intolerable delay and make the rest of the packets be transmitted with a reasonable delay. Generally, the threshold of the tolerable delay is $0.05s$. In the later simulation, any VoIP packet with delay larger than $0.05s$ will be dropped.

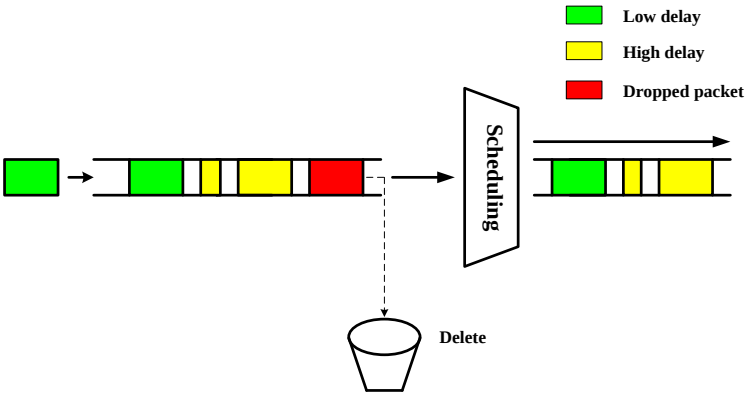

Figure 6.1: *Drop packet with large delay*

The metrics to evaluate QoS of VoIP service are the packet loss rate, the total number of served VoIP calls and the delay of the VoIP calls. The packet loss rate mainly decides whether a VoIP service can be served or not. Generally, if a VoIP call needs to be served, the packet loss rate should not be higher than 5%. In this section, both the packet loss rate of each VoIP call and the packet loss rate of all the VoIP calls are of interest. In addition, the VoIP user's experience also depends on the delay of the VoIP call. Therefore, it is also interesting to see the distribution of the packet delay. In this section, the Empirical Cumulative Distribution Function (ECDF) is chosen as the criterion. The definition of ECDF is rewritten as following:

$$F_{emp.}(y) = \frac{1}{n} \cdot \sum_{i=1}^{n} 1_{\{y_i \leq y\}}, \tag{6.1}$$

where n represents the number of a set of observations $y_1, y_2, ..., y_n$. Generally, the packet loss rate is the main issue to measure the performance of scheduling schemes. The lower packet loss rate and the larger amount of supported VoIP calls the better overall network performance it will be. Besides this, it is also better if a larger percentage of the packets are with small delays. In addition, since the GPS introduces position errors while locating MSs [48], the impact of employing positioning system should also be taken into account.

6.3 Evaluation schemes

For the evaluation of the proposed scheme, system level simulations are run on the platform – OMNet++ [49]. In order to provide a good comparison for the proposed scheme, the uniform power mask with frequency reuse of one and uniform power mask with frequency reuse of two are chosen, meanwhile, the local scheduler at BS applies the same local scheduling scheme – the FIFO scheme in previous chapter. For the proposed ASFR, the impact of different generation numbers and different objective functions (different channel capacity estimations) of GA as well as different distributions of traffic load should be investigated. Here, a list of acronyms for the comparison schemes is given as below:

Scheme name	Acronym
Uniform power mask with frequency reuse 1	Uniform reuse 1
Uniform power mask with frequency reuse 2	Uniform reuse 2
ASFR with naive capacity estimation	ASFR Naive
ASFR with static capacity estimation	ASFR Static
ASFR with dynamic capacity estimation	ASFR Dynamic

Table 6.1: *Acronyms for simulation schemes*

6.4 Simulation parameters & scenario descriptions

6.4.1 Load description and simulation parameters

The traffic load of the simulation is dependent on the number of VoIP flows as well as the VoIP packet inter-arrival time. In all the simulations, it is assumed each MS establishes only one VoIP call, but a smaller VoIP packet inter-arrival time ($1ms$) is chosen in order to increase the traffic load; for Adaptive Multi-Rate audio codecs (AMR), the VoIP inter-arrival time is $20ms$, which means each MS with VoIP $1ms$ packet inter-arrival time is a super MS and represents roughly 20 common MSs.

Moreover, it is also important to observe the queue with steady state. Otherwise, it is a risk that result comes from transient state which may offer lower packet loss rate and smaller packet delay. In order to reduce the transient queue state, the

simulation runs with a relatively long duration. It is found a suitable simulation time can be achieved with $6s$ simulation time and the simulation result is stable.

The simulation parameters is shown in Table 6.2.

Parameter	Assumption
Cellular layout.	2 cells, 1 sector per cell
Center frequency / Bandwidth	2 GHz / 5 MHz(25 RBs)
Inter-site distance	500 m
Overall transmission power	43 dBm
Frame duration	1 ms
Symbols per frame	7
SINR to Capacity	See Table A.1
Noise power	10^{-10} W
Path loss model	$L = 128.1 + 37.6 \cdot \log_{10}(R)(dB)$, R in kilometers [50]
Fading model	Rayleigh fading, delay spread 0.15μs
VoIP packet inter-arrival time	1 ms
VoIP packet size	288 bits
VoIP silence packet size	32 bits
Packet dropping threshold	50 ms

Table 6.2: *Simulation parameters*

6.4.2 Simulation factors

GA convergence

In this scenario, the aim of simulation is to find out a suitable generation number for GA. This is because for different GA parameters – crossover probability, mutation probability, population size, replacement percentage and flush frequency – GA needs different generations to converge. In Section 4.3, the minimum rate in the system is dependent on the power masks and RB assignment prediction, and therefore, GA has a transient status before finding the real performance score of any random generated power mask. This means it is not helpful to use an intermediate power mask score to represent its power mask performance before GA converges. Therefore, it is important to first find the right generation number for the later coming simulations. Table 6.3 shows the basic parameter setting of GA. In this section, the suitable generation number for ASFR Dynamic, ASFR

Parameter	Assumption
Crossover method	One-point crossover
Crossover probability	0.9
Mutation method	Flip Mutation
Mutation probability	0.001
population size	10
replacement percentage	0.8%
flush frequency	50

Table 6.3: *GA parameters*

Static and ASFR Naive is found. The generation number is dependent on the convergence of GA. A suitable generation number should guarantee that the score for evaluation of chromosomes converges. Therefore, simulations are first executed with 15000 generation number for different schemes. Figure 6.2 shows the scores of different generation number for different schemes and illustrates it is sufficient for GA to converge with 15000 generation number for all the three schemes. In the following simulations, 15000 generation number is the basic setting for GA.

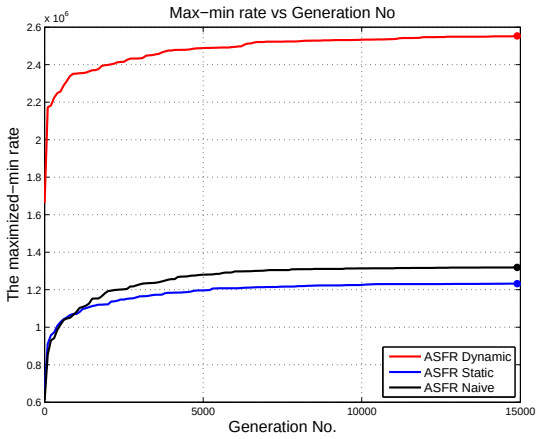

Figure 6.2: *Generation number for GA to converge*

Impact of different capacity estimations

In order to compare the impact of different capacity estimations, simulations should run with different capacity estimation functions. Figure 6.3 and Figure

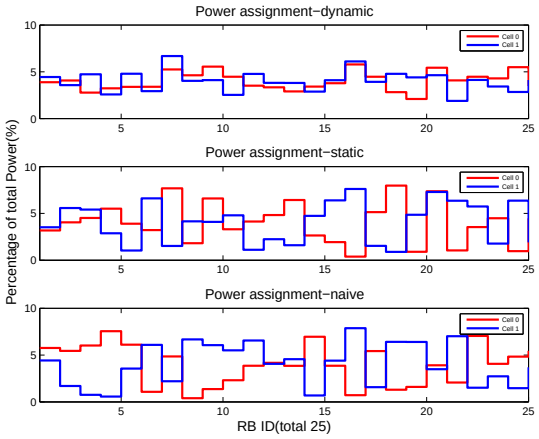

Figure 6.3: *Power assignment of different capacity estimations*

6.4 show the power masks generated by different channel capacity estimations and its corresponding performance respectively. The packet loss rate of ASFR Dynamic, ASFR Naive and ASFR Static is about $4\%, 7.8\%$ and 7.1% respectively. It is clear from the results that the ASFR Dynamic is outperforming ASFR Static and ASFR Naive; it reduces the total packet delay and the overall packet loss rate significantly. Therefore, in the later simulation, the ASFR Dynamic is chosen for the main scheme to compare with the well-known schemes.

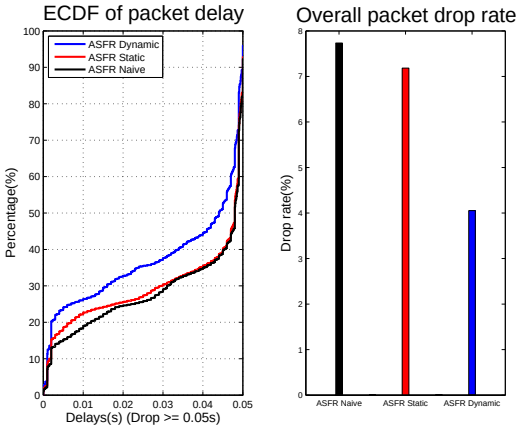

Figure 6.4: *Performance of different capacity estimations*

6.4.3 Simulation scenarios

Since the proposed ICI coordination scheme highly depends on the positions of MSs and the MS's position does not change a lot within a short time span, it is important to investigate its performance with fixed MSs. In order to compare the performance of the proposed ICI coordination scheme with other general schemes, different geographical distributions of MSs are to be used.

In this section, the investigation is based the comparison with different schemes of a reference traffic load which guarantees BSs serve the VoIP calls with packet loss rate around 5%. The uniform reuse 1 scheme with a reference traffic load is taken as the reference scheme. In order to find a good reference traffic load for different distribution scenarios, simulations first start with a given distribution M of a MS group that all the VoIP calls are able to be supported by uniform reuse 1 scheme. Then there is another number of MSs which are dropped into the simulation geographical area one by one according to the distribution rule until one or some of them start to have a packet loss rate around 5%. Then the number of the MSs and their geographical distribution is taken as the reference traffic load. All the rest of the schemes are going to run the simulations with the reference traffic load.

In order to find the impact of the different traffic distribution on GA, the MSs are only distributed on a straight line that connects two BSs. In this way, the impact of interference is still kept without loss of generality. Simulations are executed with different kinds of traffic distribution on the line.

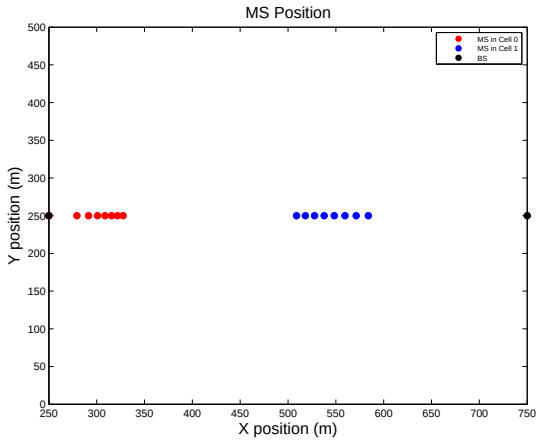

Figure 6.5: *MS position: center-edge distribution*

Center and edge distributed scenario

In this scenario, a cell is divided into three parts: cell-center area, cell-intermediate area and cell-edge area. The simulations run with the condition that a group of MSs are uniformly distributed within the border area in one cell, but a group of MSs are uniformly distributed at the center area in another cell. For this specified geographical distribution, only the MSs close to the cell border are suffering from the ICI a lot, and the other group of MSs has relative good channel states. In Figure 6.5, the location of MSs according to the description is shown. In Figure

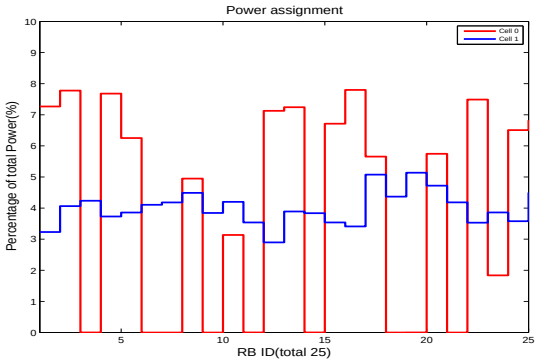

Figure 6.6: *Power assignment: center and edge distribution*

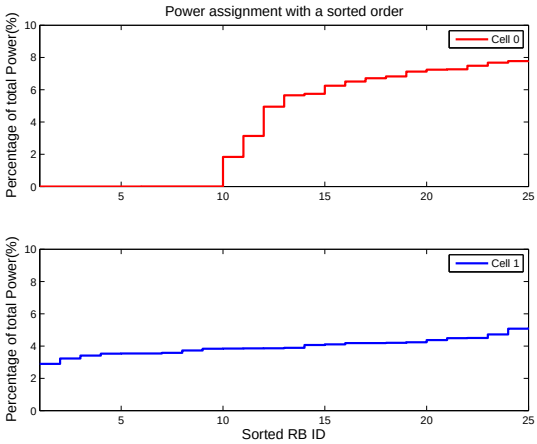

Figure 6.7: *Sorted power assignment: center and edge distribution*

6.6, the power mask generated by ASFR Dynamic scheme is shown, and Figure 6.7 shows the power allocation in ascending order. From the power mask, it can be known that the ASFR detects the right cell of high traffic load and the interference

has high impact on the performance of the right cell and simultaneously the left cell has low traffic load and there is slight interference; the central entity switches off some RBs in the left cell and keeps the power close to uniform distributed in the right cell. By this power allocation, although the power for some of the RBs is increased, the available bandwidth in the left cell is reduced and, for the right cell, some RBs have very good channel status because of no or little interference. The ECDF of packet delay and overall packet loss rate during the whole simulation time are shown in Figure 6.8. For ASFR Dynamic scheme, about 80% packet have the delay of no more than $0.017s$ and the overall system packet loss rate is about 1.4%, but considered with uniform reuse 1 and uniform reuse 2, it is about 60% and 47% packets respectively for the same packet delay threshold and the overall system packet loss rate is about 3.8% and 18.8% respectively; it can be seen that the ASFR Dynamic scheme has better performance than uniform reuse 1 and uniform reuse 2 either for the ECDF of total packet delay or system packet loss rate. The uniform reuse 2 scheme has the worst performance; this is because the reduced available bandwidth. The ASFR Dynamic scheme has better than uniform reuse 1 because it shifts the extra capacity from the cell of the low traffic load to the one of high traffic load.

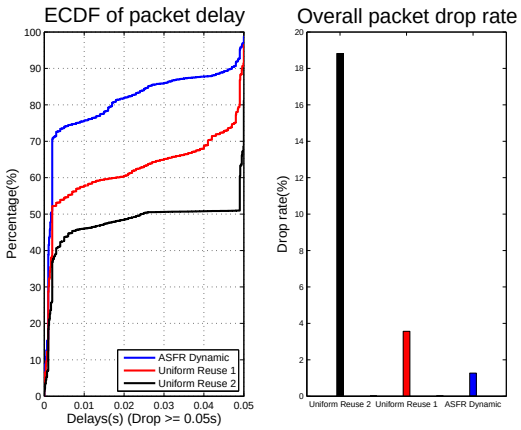

Figure 6.8: *Performance: center and edge uniform area distribution*

Full-scale and center distributed scenario

In this scenario, the simulation run with a traffic distribution that, in one cell, a group of MSs are uniformly distributed within the left cell, and a group of MSs are uniformly distributed within the cell-center area, in the right cell. For this kind of traffic load distribution, only a small number of MSs at cell-edge of the

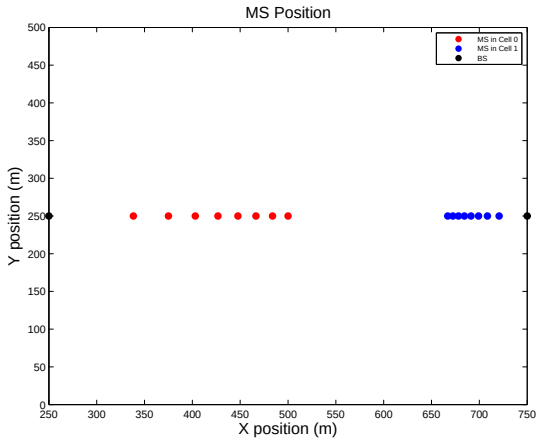

Figure 6.9: *MS position: full-scale and center distribution*

left cell are suffering from the interference. The MSs in the right cell almost have no significant interference. The geographical distribution is shown as Figure 6.9. The proposed ASFR Dynamic scheme provides the power mask as Figure

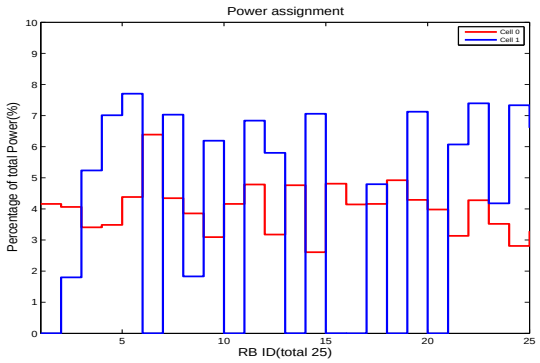

Figure 6.10: *Power assignment: full-scale and center distribution*

6.10 and Figure 6.11 shows the power allocation in ascending order. From the power mask, it can be known that the ASFR detects the left cell of high traffic load and the interference has high impact on the performance of the left cell and simultaneously the right cell has low traffic load and there is slight interference; the central entity switches off some RBs in the right cell and keeps the power close to uniform distributed in the left cell. The corresponding performance is shown as Figure 6.12. The differences of the performance are very obvious; for ASFR Dynamic scheme, about 80% packet have the delay of no more than $0.013s$ and the overall system packet loss rate is about 0.3%, but considered with uniform reuse 1 and uniform reuse 2, it is about 52% and 38% packets respectively for the same

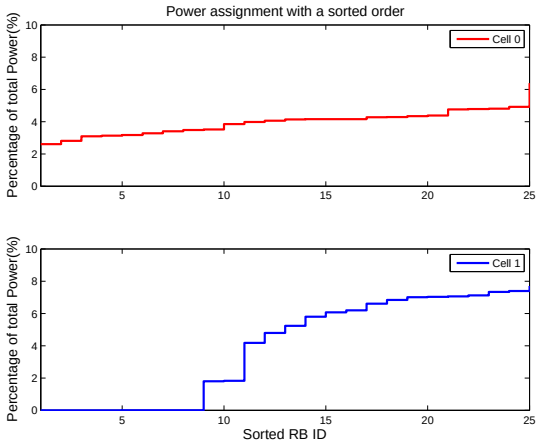

Figure 6.11: *Sorted power assignment: full-scale and center distribution*

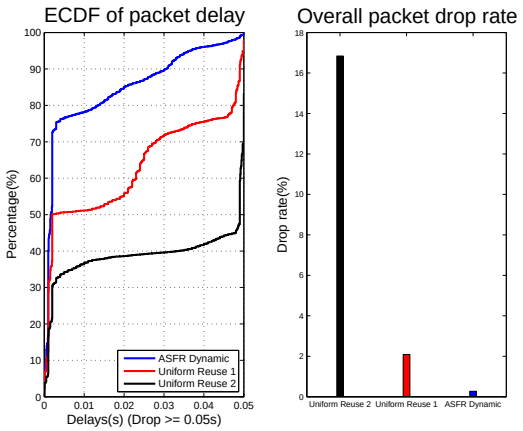

Figure 6.12: *Performance: full-scale and center uniform area distribution*

packet delay threshold and the overall system packet loss rate is about 2.1% and 16.8% respectively. ASFR Dynamic scheme has significant system performance improvement compared with uniform reuse 1 and uniform reuse 2. The proposed ASFR scheme is still able to perform ICI coordination very well.

Full-scale and edge distributed scenario

In this scenario, the simulation run with a traffic distribution that, in one cell, a group of MSs are uniformly distributed within the left cell, and in the right cell, a group of MSs are uniformly distributed within the cell-edge area. For this kind of traffic load distribution, only the part of MSs at cell-edge of the left cell are suffering

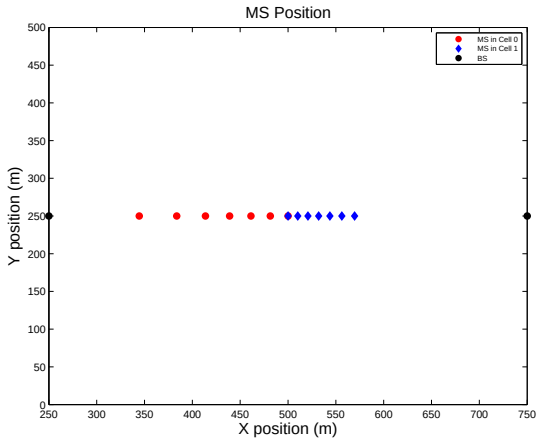

Figure 6.13: *MS position: full-scale and edge distribution*

from the interference. All the MSs in the right cell have significant interference coming from the left cell. The geographical distribution is shown as Figure 6.13.

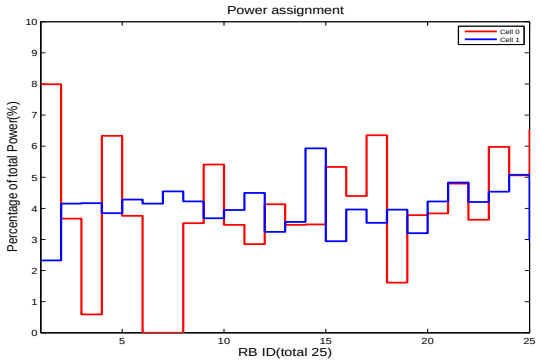

Figure 6.14: *Power assignment: full-scale and edge distribution*

The power mask generated by ASFR Dynamic scheme is illustrated by Figure 6.14 and Figure 6.15 shows the power allocation in ascending order. From the power mask, it shows that only few RBs of the left cell are switched off; the ASFR is still able to detect low traffic load cell and shift the capacity to the cell of high traffic load. In Figure 6.16, the performance of proposed scheme, uniform reuse 1 and uniform reuse 2 are shown. For ASFR Dynamic scheme, about 80% packet have the delay of no more than 0.048s and the overall system packet loss rate is about 3.7%, but considered with uniform reuse 1 and uniform reuse 2, it is about 74% and 45% packets respectively for the same packet delay threshold and the overall system packet loss rate is about 4% and 24.2% respectively. ASFR Dynamic scheme has better system performance improvement compared with uniform reuse

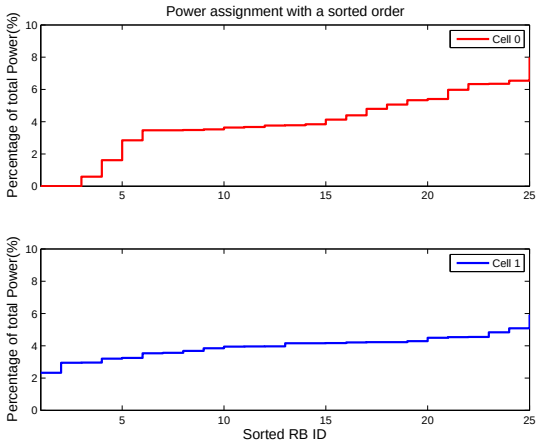

Figure 6.15: *Sorted power assignment: full-scale and edge distribution*

1 and uniform reuse 2, although the difference between ASFR Dynamic scheme and uniform reuse 1 is not significant. The proposed ASFR scheme is still able to perform ICI coordination well.

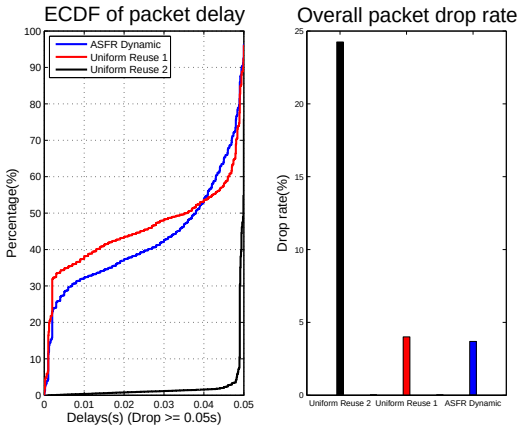

Figure 6.16: *Performance: full-scale and edge uniform area distribution*

Center and center distributed scenario

In this scenario, the traffic distribution is that, in both of the two cells, there is a group of MSs uniformly distributed within the center area. For this kind of distribution, there is almost no significant interference. The geographical distribution is shown as Figure 6.17. Figure 6.18 illustrates the power mask generated by

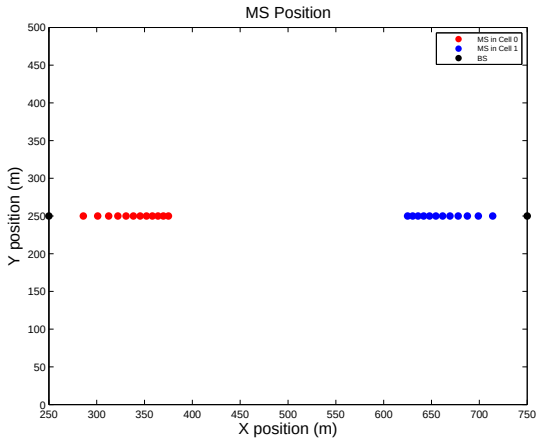

Figure 6.17: *MS position: center and center distribution*

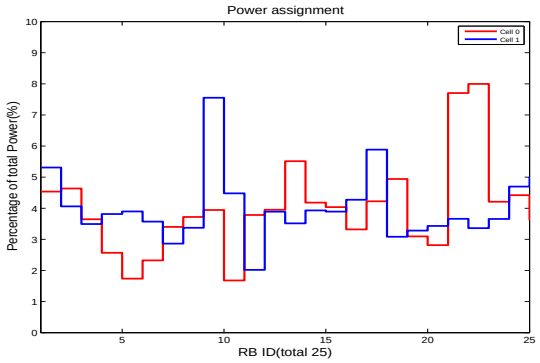

Figure 6.18: *Power assignment: center and center distribution*

ASFR Dynamic scheme and Figure 6.19 shows the power allocation in ascending order and Figure 6.20 shows the performance of this scheme compared with the other well-known schemes. From the simulation results, it shows that ASFR Dynamic and uniform reuse 1 have almost the same performance and both of them are better then uniform reuse 2. Since there is little impact of ICI and all MSs close to the BS have very good channel status, it can be expected that the slight variance of the transmit power affects the system performance. The reduction of system bandwidth significantly degrades the system performance for this low ICI traffic load distribution, and that is the main reason why uniform reuse 2 has so bad performance.

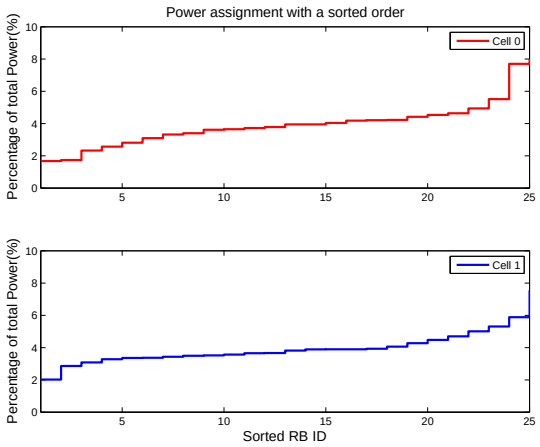

Figure 6.19: *Sorted power assignment: center and center distribution*

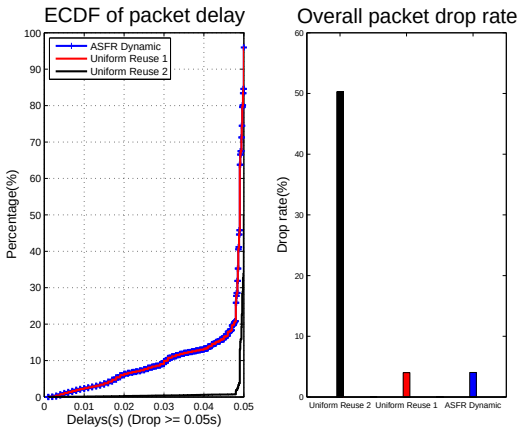

Figure 6.20: *Performance: center and center uniform area distribution*

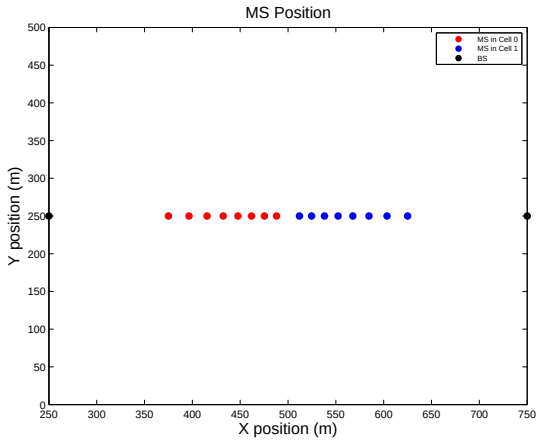

Figure 6.21: *MS position: edge and edge distribution*

Edge and edge distributed scenario

In this scenario, the simulations run with a group of MSs with specified geographical locations; all the MSs are distributed close to the border in both cells, which means this scenario makes all the MSs suffer from the ICI a lot. The geographical distribution is shown as Figure 6.21. Figure 6.23 shows the power allocation

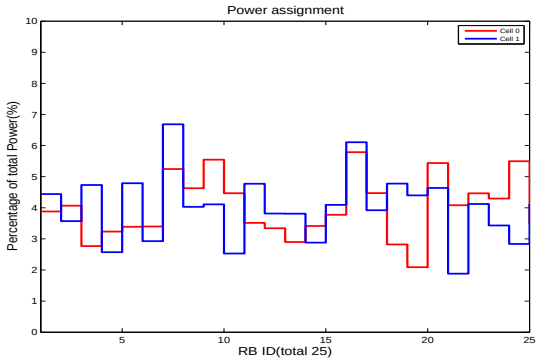

Figure 6.22: *Power assignment: edge and edge distribution*

in ascending order. The power mask and performance of ASFR Dynamic scheme is shown as Figure 6.22 and Figure 6.24 respectively. From the performance results, it shows that for this symmetric traffic distribution, ASFR Dynamic and uniform reuse 1 have very close performance, even uniform reuse 1 has a little better performance, but both of them have better performance than uniform reuse 2.

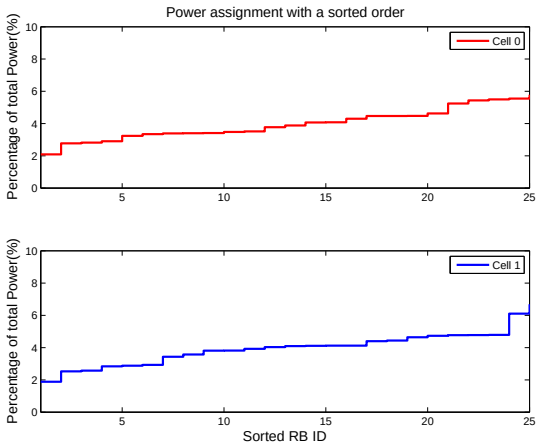

Figure 6.23: *Sorted power assignment: edge and edge distribution*

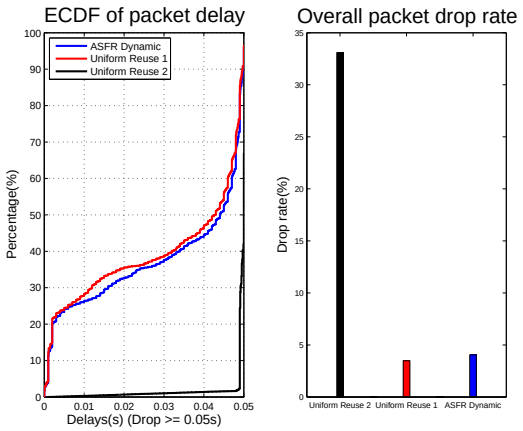

Figure 6.24: *Performance: edge and edge uniform area distribution*

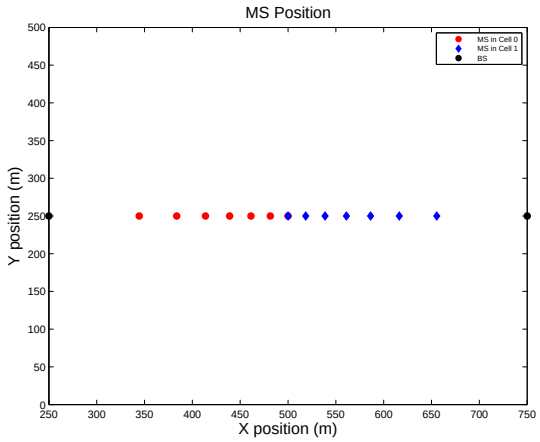

Figure 6.25: *MS position: distribution*

Full-scale distributed scenario

In this scenario, there is a group of MSs uniformly distributed within the whole cell area for both of the two cells. For this kind of distribution, there are some MSs which almost suffer no significant ICI and there are also some MSs which suffer ICI a lot. The geographical distribution is shown as Figure 6.17. The

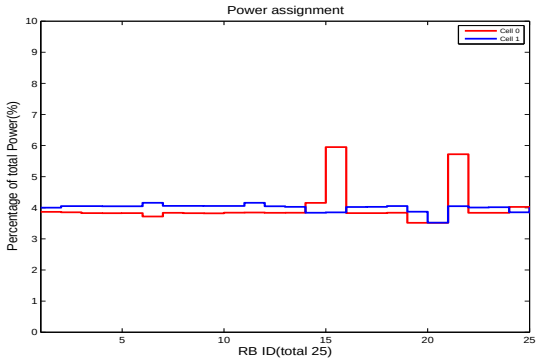

Figure 6.26: *Power assignment: Full-scale distribution*

power mask of ASFR Dynamic is illustrated in Figure 6.26 and Figure 6.27 shows the power allocation in ascending order. From the power mask, it can be shown that the power mask generated by ASFR Dynamic is very close to uniform reuse 1. The performance of different schemes are shown in Figure 6.28. The overall packet loss rate is $0.36\%, 0.41\%$ and 21.3% for ASFR Dynamic, uniform reuse 1 and uniform reuse 2 respectively. It can be found that ASFR Dynamic has very

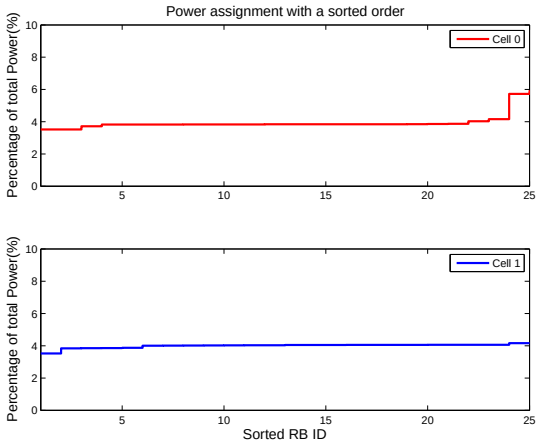

Figure 6.27: *Sorted power assignment: Full-scale distribution*

similar performance with uniform reuse 1 from the ECDF of packet delay, but ASFR Dynamic has a litter bit lower overall packet loss rate. Furthermore, the uniform reuse 2 still has the worst performance.

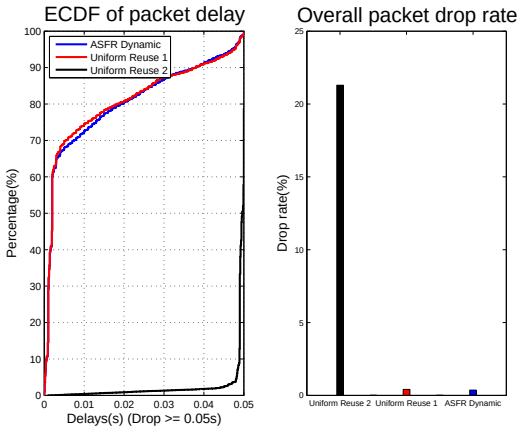

Figure 6.28: *Performance: Full-scale distribution*

6.4.4 Employing propagation maps

After previous investigations, it is interesting to see what is the performance if the path loss channel model is replaced by the realistic propagation environment. Therefore, two propagation maps are employed for the later coming investigations. Since the inter-cell distance is changed to be around $700m$, the packet inter-arrival time is modified to be 2ms, in order to avoid the system only severing very few MSs. The other simulation settings are still kept the same. Then the simulations with previous distributions are executed again for ASFR Dynamic, uniform reuse 1 and uniform reuse 2. Moreover, it is known that while GPS is employed, the deviation of it is also introduced. That means the average channel gain obtained by GA is erroneous. Therefore, it is also interesting to see what the performance the GA has with the erroneous channel information. In the follow simulations, the ASFR Dynamic scheme using erroneous average channel gain is called **ASFR Dynamic-E** for short.

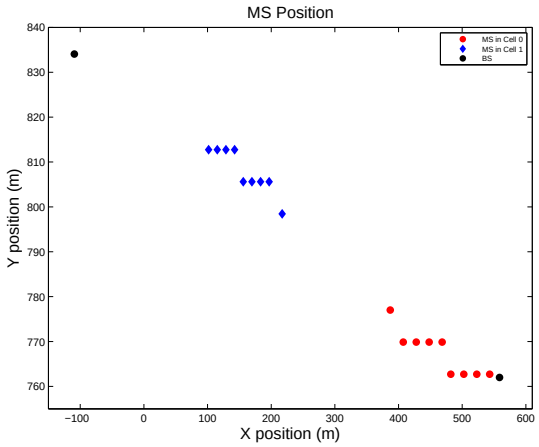

Figure 6.29: *MS position for propagation maps: center-edge distribution*

Center and edge distributed scenario

In this scenario, the distribution of MSs are as Figure 6.29 shown; in the left cell, MSs are all close to the cell border, and in the right cell, MSs are all close to cell center. The Root Mean Square Error (RMSE) of using erroneous average channel gain is 0.3642 dB. The power mask generated by ASFR Dynamic scheme using correct or erroneous average channel gain is illustrated in Figure 6.30. It is obvious that ASFR Dynamic scheme knows that the left cell has high traffic load and the right cell has extra capacity and therefore some of the RBs are switched off in the

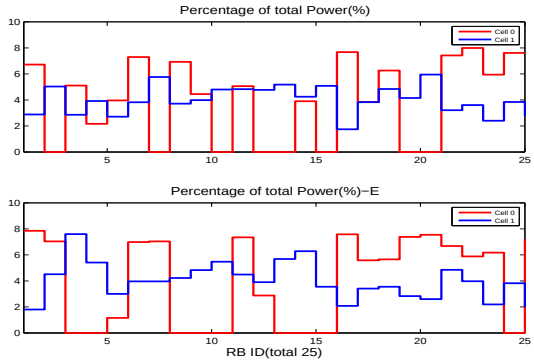

Figure 6.30: *Power assignment for propagation maps: center-edge distribution*

right cell in order to improve the channel status of the left cell. The performance results of this scenario is shown as Figure 6.31. For ASFR Dynamic scheme using either correct average channel gain or erroneous one, 100% of all the packets has delay no more than 0.01s, and for uniform reuse 2 and uniform reuse 1, about 94% and 58% of all the packets have delay lower than the same delay threshold. Moreover, ASFR Dynamic scheme and uniform reuse 2 has not packet loss rate at all, but uniform reuse 1 has overall loss rate about 4.9%. It is clear that ASFR Dynamic scheme is outperforming the other schemes. uniform reuse 1 has the worst performance; it has the largest overall packet delay and the largest packet loss rate. In addition, the negative impact of using the erroneous average channel gain can hardly be seen from the ECDF of packet delay and the overall packet loss rate. This is because the average channel gains of two close positions are highly correlated and they have no significant difference.

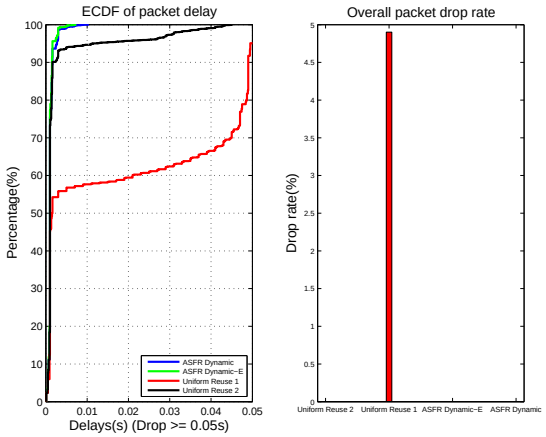

Figure 6.31: *Performance for propagation maps: center-edge distribution*

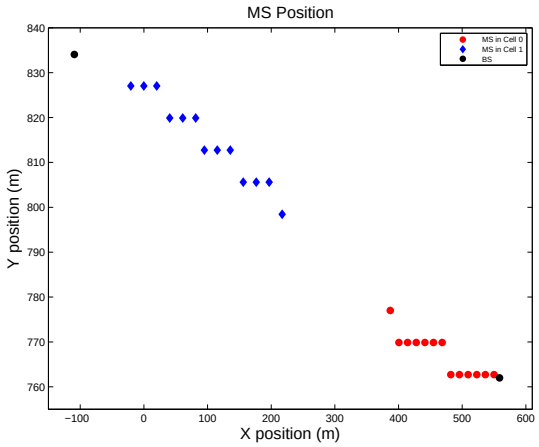

Figure 6.32: *MS position for propagation maps: uniform-center distribution*

Full-scale and center distributed scenario

In this scenario, Figure 6.32 shows the distribution of traffic: in left cell, MSs are distributed roughly uniformly along the line, and in the right cell, MSs are all close to the BS. The RMSE of using erroneous average channel gain is 0.4235 dB. Figure 6.33 shows the power masks given by ASFR Dynamic scheme using correct and erroneous average channel gain. The performance of different schemes are

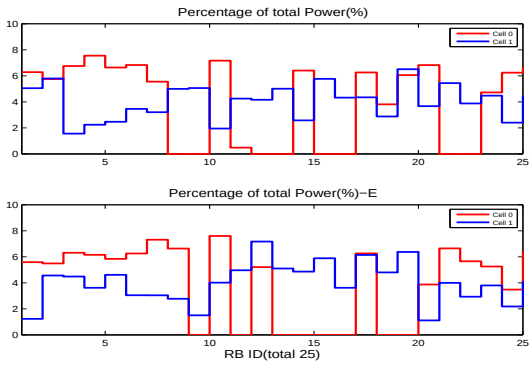

Figure 6.33: *Power assignment for propagation maps: uniform-center distribution*

illustrated in Figure 6.34. For ASFR Dynamic scheme, above 90% packets have delay smaller than 0.01s and there is no packet loss during the whole simulation. However, for uniform reuse 1 and uniform reuse 2, about 61% and 6% packets have delay smaller than the same threshold respectively, and the overall packet loss rate is about 6.4% and 16% respectively. It is obvious that the ASFR Dynamic scheme

has the best performance. In addition, there is almost no negative impact of using the erroneous average channel gain.

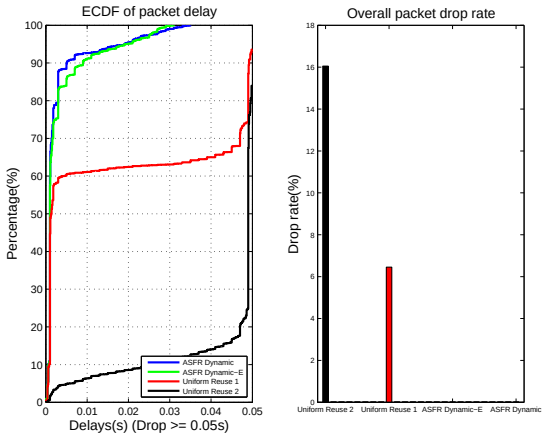

Figure 6.34: *Performance for propagation maps: uniform-center distribution*

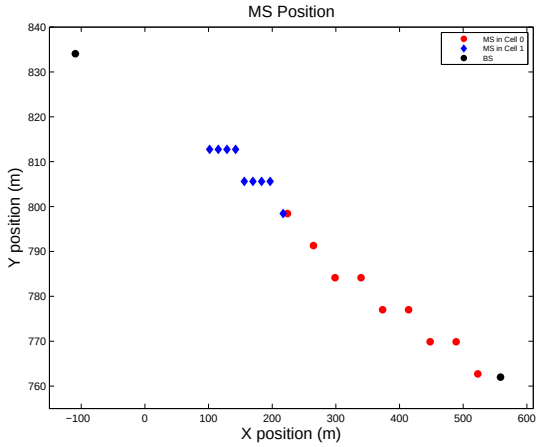

Figure 6.35: *MS position for propagation maps: uniform-edge distribution*

Full-scale and edge distributed scenario

In this scenario, the traffic distribution is shown in Figure 6.35. In the left cell, the traffic is close to the cell border and in the right cell, MSs are uniformly distributed along the line. The RMSE of using erroneous average channel gain is 0.2582 dB. Figure 6.36 shows the power masks provided by ASFR Dynamic using correct and erroneous average channel gain. The performances of all simulated schemes are

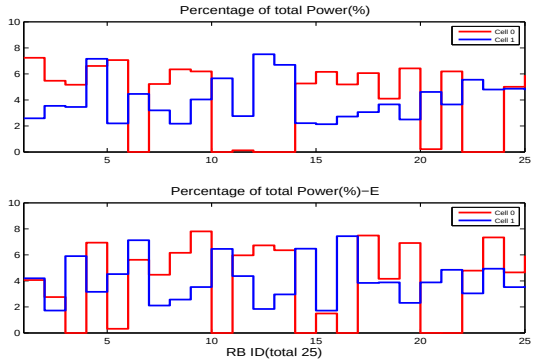

Figure 6.36: *Power assignment for propagation maps: uniform-edge distribution*

shown in Figure 6.37. It shows that for ASFR Dynamic scheme and uniform reuse 2 have about 95% packets of delay smaller than $0.01s$ and both of them have no packet loss duration the whole simulation, but uniform reuse 1 only has 58% packets of delay smaller than the same delay threshold and it has packet loss rate about 4.9%. Moreover, the ASFR Dynamic scheme has a little better performance than uniform reuse 2 from the ECDF of packet delay. In addition, the negative impact of using the erroneous average channel gain is very small.

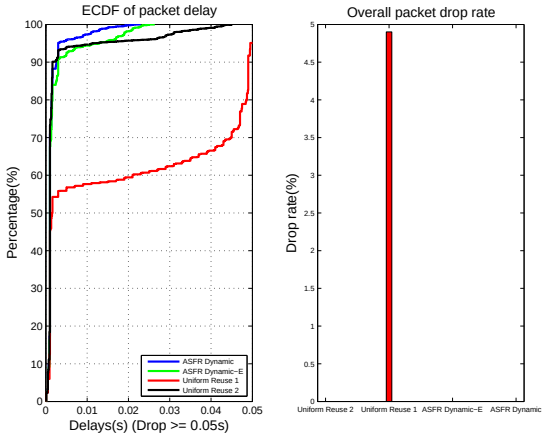

Figure 6.37: *Performance for propagation maps: uniform-edge distribution*

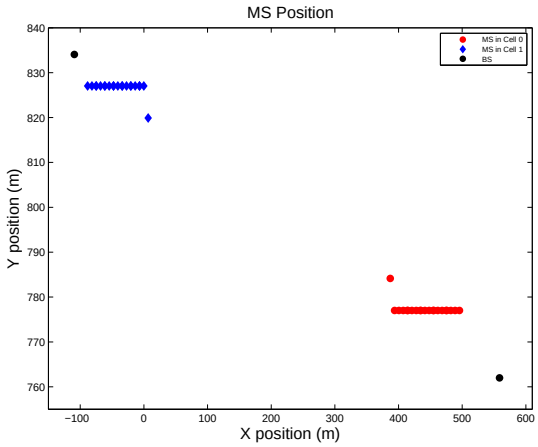

Figure 6.38: *MS position for propagation maps: center-center distribution*

Center and center distributed scenario

In this scenario, the traffic distribution is illustrated in Figure 6.29. For both cells, all the MSs are close to the BS. The RMSE of using erroneous average channel gain is 0.2833 dB. In Figure 6.39 shows the power masks provided by ASFR Dynamic scheme using correct and erroneous average channel gain.

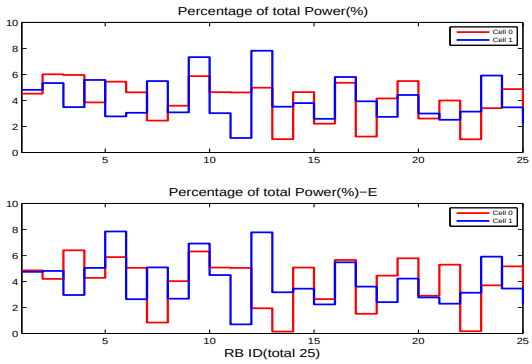

Figure 6.39: *Power assignment for propagation maps: center-center distribution*

The performances of all the schemes are shown in Figure 6.40. The uniform reuse 1 and ASFR Dynamic scheme have very close performance. This is because all the MSs are close to the cell center and, therefore, there is almost few impact of ICI from the other cell and MSs have very good channel status. uniform reuse 2 has the worst performance because of the shortage of bandwidth. The negative impact of using erroneous average channel gain is very small.

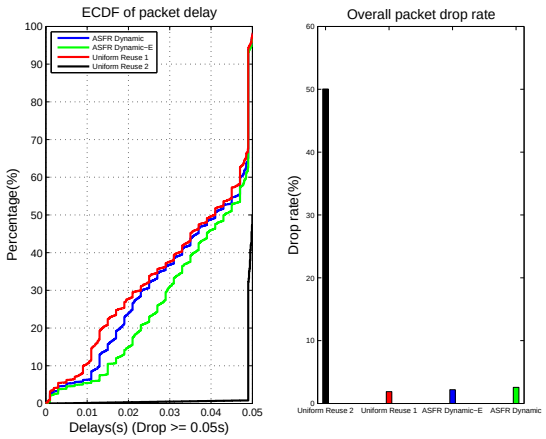

Figure 6.40: *Performance for propagation maps: center-center distribution*

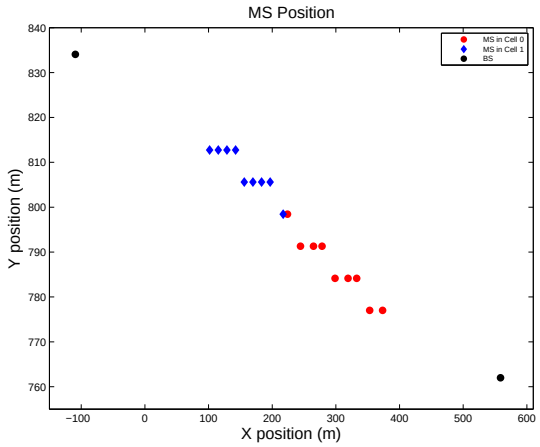

Figure 6.41: *MS position for propagation maps edge-edge distribution*

Edge and edge distributed scenario

In this scenario, the traffic distribution is shown in Figure 6.41: both of the cells have MSs close to cell edge. The RMSE of using erroneous average channel gain is 0.2402 dB. The power mask provided by ASFR Dynamic scheme using correct or erroneous average channel gain is illustrated in Figure 6.42. The performance of each scheme is illustrated in Figure 6.43. For this traffic distribution, the performance of ASFR Dynamic scheme is very close to the one of uniform reuse 2 – above 90% packet have delay smaller than 0.01s and there is no packet loss during whole simulation, but both of them have significant performance improvement than uniform reuse 1, which only has about 58% packet of delay smaller than 0.01s and whose overall packet loss rate is about 4.9%. This is because the ICI is mitigated

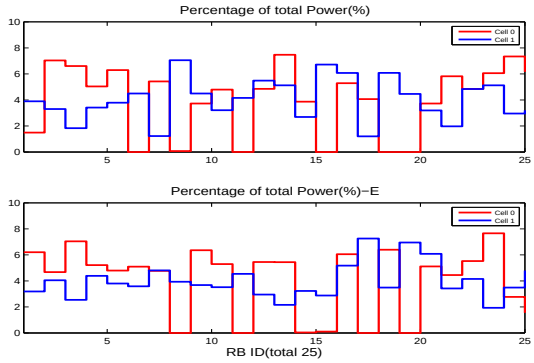

Figure 6.42: *Power assignment for propagation maps: edge-edge distribution*

by ASFR Dynamic, and for uniform reuse 2, there is no ICI. In addition, the negative impact of using the erroneous average channel gain can not be seen from the ECDF of packet delay and the overall packet loss rate, even ASFR Dynamic-E has the best performance.

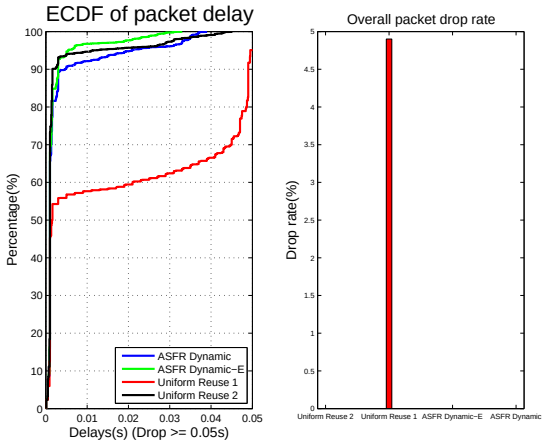

Figure 6.43: *Performance for propagation maps: edge-edge distribution*

Full-scale distributed scenario

In this scenario, simulation is executed with a traffic load that in both cells MSs are uniformly distributed along the line that connected with the two BSs, see 6.44. The RMSE of using erroneous average channel gain is 0.2779 dB. The power mask generated by ASFR Dynamic scheme using correct or erroneous average channel gain is as Figure 6.45 shown. The ECDF of packet delay and overall packet loss rate

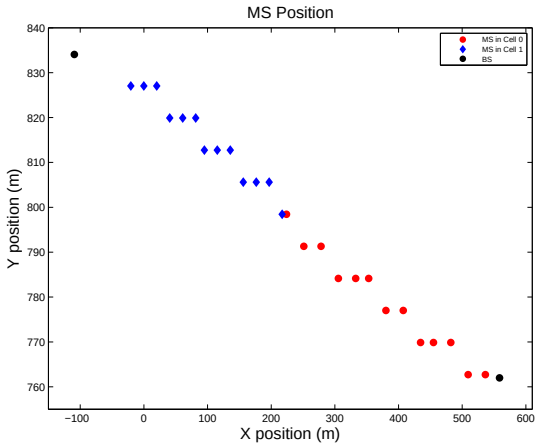

Figure 6.44: *MS position for propagation maps: full-scale distribution*

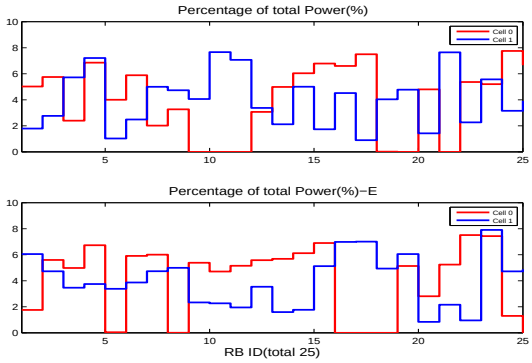

Figure 6.45: *Power assignment for propagation maps: full-scale distribution*

are illustrated in Figure 6.46. Since the propagation environment is not symmetric in the propagation maps, the traffic load is not symmetric anymore even if the MS distribution is symmetric. Therefore ASFR Dynamic shifts the capacity from the low load cell to the high load one by switching off some RBs in the low load cell to improve the channel status in the high load cell. The performance of ASFR Dynamic scheme is much better than the other two schemes. Still, there is no negative impact of using the erroneous average channel gain.

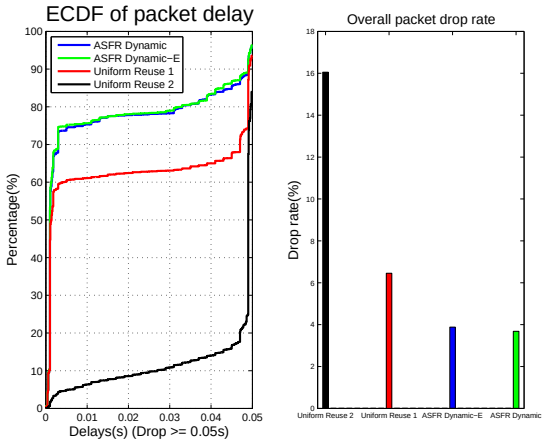

Figure 6.46: *Performance for propagation maps: full-scale distribution*

Chapter 7

Summary

The main objective of the thesis is to find a good ASFR scheme with employing the propagation maps for ICI coordination in LTE system. The proposed ASFR scheme is designed to be able to adapt to change of the traffic distribution and improve the system performance. In this thesis, the ICI coordination is modeled to maximize the minimum estimated data rate in the system for VoIP service and GA are employed in order to solve the optimization problem; in this way, the proposed scheme takes the MSs of bad channel status into account and performs ICI coordination.

From the evaluation of the convergence of GA, it shows that GA needs a sufficient computation in order to solve the optimization problem. This is because the solution GA is based on the evolution of random numbers. Therefore, the convergence of GA guarantees the reliability of sub-optimal solution. The higher iteration number that GA provides more reliable solution close to the optimal one.

From the evaluation of the impact of different capacity estimation methods, it can be concluded that the frequency diversity gain of RB allocation has high impact on the prediction of channel capacity and using a good capacity estimation can significantly improve the power mask performance provided by GA and therefore the ICI coordination performance is dependent on the capacity estimation function. This is because the proposed scheme separates the ICI coordination and local scheduling into two parts in order to grant the local scheduler the freedom of RB allocation; this allows the local scheduler to exploit the channel diversity gain without restrictions coming from the ICI coordination; however, for the prediction of data rate, the traditional way to calculate the capacity is only based on the SINR which does not consider the frequency diversity gain that a local scheduler

is able to exploit. Therefore, the impact of the frequency diversity gain should be taken into account when ICI coordination is performed in the proposed model.

From the evaluation of the different traffic distributions by comparison with Uniform Reuse 1 and Uniform Reuse 2, it can be concluded that if the traffic follows an asymmetric distribution, the proposed ASFR scheme can distinguish different traffic load and provide good power masks for ICI coordination; it not only reduces the packet delay but also reduces the packet loss rate. If the traffic distribution is symmetric, then the proposed ASFR scheme can provide similar performance with Uniform Reuse 1 but not significantly outperform it. Uniform Reuse 2 has the worst performance, which is because of the shortage of bandwidth. Considering the realistic propagation environment, generally, the traffic load is asymmetric because of asymmetric propagation environment of different cells and that is the reason why ASFR scheme outperforms Uniform Reuse 1 and Uniform Reuse 2 if employing the propagation maps. Moreover, from the simulation results of using erroneous average channel gain, it can be concluded that the error introduced by the positioning technology and even any factors (such as inaccuracy due to the change of shadowing) that leads to erroneous average channel gain has very small negative impact on the ICI coordination performance.

As the thesis only investigates the ASFR scheme for two-cell scenario, it still needs further investigations for multi-cell scenario and research of how to describe the channel capacity with consideration of frequency diversity gain for multiple cells. Moreover, in order to improve the computation speed of GA to solve the optimization problem, further research should be done, such as grouping the MSs and parallel computing.

Bibliography

[1] X. Y. Zhang, C. He, L. G. Jiang, and J. Xu, "Inter-cell interference coordination based on softer frequency reuse in OFDMA cellular systems," June 2008, IEEE International Conference on Neural Networks and Signal Processing.

[2] A. Hernandez, I. Guio, and A. Valdovinos, "Interference Management through Resource Allocation in Multi-Cell OFDMA Networks," April 2009, IEEE 69th Vehicular Technology Conference.

[3] "S. R0023, High Speed Data Enhancement for CDMA2000 1x-Data Only," 3GPP2, June 2000.

[4] "High Speed Downlink Packet Access (HSDPA), Release 5," 3GPP, 2003.

[5] 3GPP TS 36.211, "3rd Generation Partnership Project; Evolved Universal Terrestrial Radio Access (E-UTRA); Physical channels and modulation, ver 8.7.0," Jun. 2009.

[6] 3GPP TR 36.814, "3rd Generation Partnership Project; Evolved Universal Terrestrial Radio Access (E-UTRA); Further advancements for E-UTRA Physical layer aspects Physical channels and modulation, ver 1.0.0," Feb. 2009.

[7] 3GPP TR 25.913 V9.0.0, "3rd Generation Partnership Project; Technical Specification Group Radio Access Network; Requirements for Evolved UTRA (E-UTRA) and Evolved UTRAN (E-UTRAN) (Release 9)," Dec. 2009.

[8] 3GPP TR 25.814 V7.1.0, "3rd Generation Partnership Project; Technical Specification Group Radio Access Network; Physical layer aspects for evolved Universal Terrestrial Radio Access (UTRA)(Release 7)," Sep. 2006.

[9] T. M. Cover and J. A. Thomas, "Elements of Information Theory," 1991, Wiley.

[10] G. Boudreau, J. Panicker, N. Guo, R. Chang, N. Wang, and S. Vrzic, "Interference coordination and cancellation for 4G networks," April 2009, IEEE Communications Magazine.

[11] M. Sternad, T. Ottosson, A. Ahlen, and A. Svensson, "Attaining both coverage and high spectral efficiency with adaptive OFDM downlinks," Oct. 2003.

[12] R. Giuliano, C. Monti, and P. Loreti, "WiMAX fractional frequency reuse for rural environments," June 2008, IEEE Wireless Communications.

[13] A. L. Stolyar and H. Viswanathan, "Self-Organizing Dynamic Fractional Frequency Reuse in OFDMA Systems," April 2008, IEEE International Conference on Computer Communications (INFOCOM).

[14] Z. Xie and B. Walke, "Enhanced Fractional Frequency Reuse to Increase Capacity of OFDMA Systems," Dec. 2009, 3rd International Conference New Technologies Mobility and Security (NTMS).

[15] S. E. Elayoubi, O. B. Haddada, and B. Fourestie, "Performance evaluation of frequency planning schemes in OFDMA-based networks," May 2008, IEEE Transactions on Wireless Communications.

[16] M. Bohge, J. Gross, and A. Wolisz, "Optimal power masking in soft frequency reuse based OFDMA networks," May 2009, European Wireless Conference.

[17] 3GPP, R1-050507, "Soft frequency reuse scheme for UTRAN," Huawei, 2005.

[18] K. Doppler, C. Wijting, and K. Valkealahti, "Interference Aware Scheduling for Soft Frequency Reuse," April 2009, IEEE 69th Vehicular Technology Conference.

[19] A. Aguiar and J. Gross, "Technical report tkn-03-007, wireless channel models," April 2003.

[20] X. W. Zhao, J. Kivinen, P. Vainikainen, and K. Skog, "Propagation characteristics for wideband outdoor mobile communications at 5.3 GHz," Apr. 2002, IEEE Journal on Selected Areas in Communications.

[21] T. S. Rappaport, "Wireless communications: Principles & practice, 2nd ed.," 2002, Prentice Hall.

[22] A. Goldsmith, "Wireless communications," 2005, Cambridge University Press.

[23] W. C. Jakes, "Microwave mobile communications," 1994, IEEE Press, Wiley Interscience.

[24] J. Sköld E. Dahlman, S. Parkvall and P. Beming, "3G Evolution HSPA and LTE for Mobile Broadband (2nd Edition)," 2008, Elsevier Ltd.

[25] 3GPP TS 36.300 V10.2.0, "3rd Generation Partnership Project; Technical Specification Group Radio Access Network; Evolved Universal Terrestrial Radio Access (E-UTRA) and Evolved Universal Terrestrial Radio Access Network (E-UTRAN); Overall description; Stage 2(Release 10)," Dec. 2010.

[26] 3GPP TS 36.211 V10.0.0, "3rd Generation Partnership Project; Technical Specification Group Radio Access Network; Evolved Universal Terrestrial Radio Access (E-UTRA); Physical channels and modulation (Release 10)," Dec. 2010.

[27] 3GPP TS 36.101, "3rd Generation Partnership Project; Technical Specification Group Radio Access Network; Evolved Universal Terrestrial Radio Access (E-UTRA); User Equipment (UE) radio transmission and reception (Release 10)," Jan. 2011.

[28] 3GPP TR 25.814 V7.1.0, "3rd Generation Partnership Project; Technical Specification Group Radio Access Network; Physical layer aspects for evolved Universal Terrestrial Radio Access (UTRA) (Release 7)," Sep. 2006.

[29] 3GPP TS 36.212 V8.3.0, "Technical specification group radio access network; evolved universal terrestrial radio access (e-utra); multiplexing and channel coding,(release 8)," May 2008.

[30] 3GPP TS 36.213 V8.5.0, "Technical specification group radio access network; evolved universal terrestrial radio access (e-utra); physical layer procedures,(release 8)," Dec. 2008.

[31] J. R. Koza, "Genetic programming: On the programming of computers by means of natural selection," 1998, Massachusetts Institute of Technology.

[32] M. Wall, "GAlib Documentation version 2.4," 1999.

[33] "http://en.wikipedia.org/wiki/genetic_algorithm#references," at 11:38 May 30 2011.

[34] L. Chen and D. Yuan, "Soft frequency reuse in large networks with irregular cell pattern: How much gain to expect?," Sept. 2009, IEEE 20th International Symposium on Personal Indoor and Mobile Radio Communications.

[35] Z. Bakhti and S.S. Moghaddam, "Inter-cell interference coordination with adaptive frequency-reuse for VoIP and data traffic in downlink of 3GPP-LTE," Oct. 2010, 4th International Conference on Application of Information and Communication Technologies (AICT).

[36] F. Pantisano and V. Corvino, "Position-based power planning for fair resource allocation in LTE-A," Sep. 2010, IEEE 21st International Symposium on Personal Indoor and Mobile Radio Communications (PIMRC).

[37] X. H. Mao, A. Maaref, and K. H. Teo, "Adaptive Soft Frequency Reuse for Inter-Cell Interference Coordination in SC-FDMA Based 3GPP LTE Uplinks," Dec. 2008, IEEE Global Communications Conference (GLOBECOM).

[38] D. Kim, J. Lee, and H. Lee, "Subband power allocation for tightly coordinated cellular systems," June 2009, First International Conference on Ubiquitous and Future Networks (ICUFN).

[39] M. Bohge, J. Gross, A. Wolisz, and M. Meyer, "Dynamic resource allocation in OFDM systems: an overview of cross-layer optimization principles and techniques," Jan. 2007, IEEE Network.

[40] W. Rhee and J. M. Cioffi, "Increase in capacity of multiuser OFDM system using dynamic subchannel allocation," May 2000, IEEE 51st Vehicular Technology Conference Proceedings.

[41] J. Gross, "Admission control based on OFDMA channel transformations," June 2009, IEEE International Symposium on a World of Wireless, Mobile and Multimedia Networks Workshops.

[42] F. Naghibi and J. Gross, "How bad is interference in IEEE 802.16e systems?," April 2010, European Wireless Conference (EW).

[43] "http://en.wikipedia.org/wiki/global_positioning_system," at 01:15 May 29 2011.

[44] J. Gross and M. Bohge, "Dynamic resource allocation in ofdm systems: an overview of cross-layer optimization principles and techniques," May 2006, Tech. rep. TKN-06-001, Telecommun. Networks Group, Technische Univ. Berlin.

[45] J. D. Parson, "Mobile radio propagation channel," 2000, John Wiley & Sons Ltd.

[46] M. Günes K. Wehrle and J. Gross, "Modeling and tools for network simulation," 2010, Springer.

[47] "UTRA-UTRAN Long Term Evolution (LTE) and 3GPP System Architecture Evolution (SAE)," 3GPP, 2009.

[48] "http://www.kowoma.de/en/gps/errors.htm," Apr. 19 2009.

[49] "http://www.omnetpp.org/pmwiki/index.php?n=main.omnetpp3," at 02:56 PM, Aug. 14 2010.

[50] 3GPP TR 25.814 V7.1.0, "Physical layer aspects for evolved Universal Terrestrial Radio Access (UTRA)," Sep. 2006.

Appendix A

Appendix

Acronyms

ASFR Adaptive Soft Frequency Reuse

AMR Adaptive Multi-Rate audio codecs

BS Base Station

CQI channel quality information

CQI Channel Quality Indication

eNB eNode B

E-UTRAN Evolved Universial Terrestrial Radio Access Network

ECDF Empirical Cumulative Distribution Function

eNB eNode

EPC Evolved Packet Core

E-UTRAN Evolved Universal Terrestrial Radio Access Network

FFR Fractional Frequency Reuse

FDD Frequency Division Duplex

FIFO First In First Out

GA Genetic Algorithm

GPS Global Positioning System

HSPA High Speed Packet Access

HFR Hard Frequency Reuse

ICI Inter-cell Interference

IP Internet Protocol

LOS line-of-sight

LTE Long Term Evolution

LTE-A Long Term Evolution Advanced

MS Mobile Station

MAC Medium Access Control

NED NEtwork Description

OFDM Orthogonal Frequency Division Multiplexing

OFDMA Orthogonal Frequency Division Multiple Access

PDCP Packet Data Convergence Protocol

PDF Probability Density Function

PHY Physical Layer

QoS Quality of Service

RB Resource Block

RAN Radio Access Network

RLC Radio Link Control

RMSE Root Mean Square Error

SC-FDMA Single-carrier Frequency Division Multiple Access

SINR Signal to Interference and Noise Ratio

SFR Soft Frequency Reuse

TTI Transmission Time Interval

TDD Time Division Duplex

VoIP Voice over Internet Protocol

WiMAX Worldwide Interoperability for Microwave Access

3G Third-Generation

3GPP the 3rd Generation Partnership Project

4G 4th Generation

SINR to Capacity Table

Referred in Table 6.2.

SINR(dB)	Capacity(bits)	SINR(dB)	Capacity(bits)
-20	0.0142	-19	0.0179
-18	0.0224	-17	0.0282
-16	0.0354	-15	0.0444
-14	0.0557	-13	0.0698
-12	0.0873	-11	0.1091
-10	0.136	-9	0.1693
-8	0.21	-7	0.2597
-6	0.3197	-5	0.3918
-4	0.4772	-3	0.5771
-2	0.6921	-1	0.8219
0	0.9651	1	1.1185
2	1.2771	3	1.4342
4	1.6642	5	1.9089
6	2.1605	7	2.4139
8	2.6657	9	2.9133
10	3.1522	11	3.3745
12	3.5914	13	3.8899
14	4.1939	15	4.5029
16	4.8118	17	5.1083
18	5.376	19	5.5992
20	5.7677	21	5.881
22	5.9473	23	5.9805
24	5.9946	25	5.999
26	5.9997	27	6
28	6	29	6
30	6		

Table A.1: *SINR to Capacity Table*

Acknowledgements

It doesn't matter if I continue to stay here or not.

The friendship is right here and it is not going to change.

It doesn't matter if you miss me or not.

The feeling is right here and it isn't going anywhere.

It doesn't matter if you are with me or not.

My hand is in your hand and I am not going to let go.

Let me embrace you or let me live in your heart to eternity.

My friends. My advisors. My family.